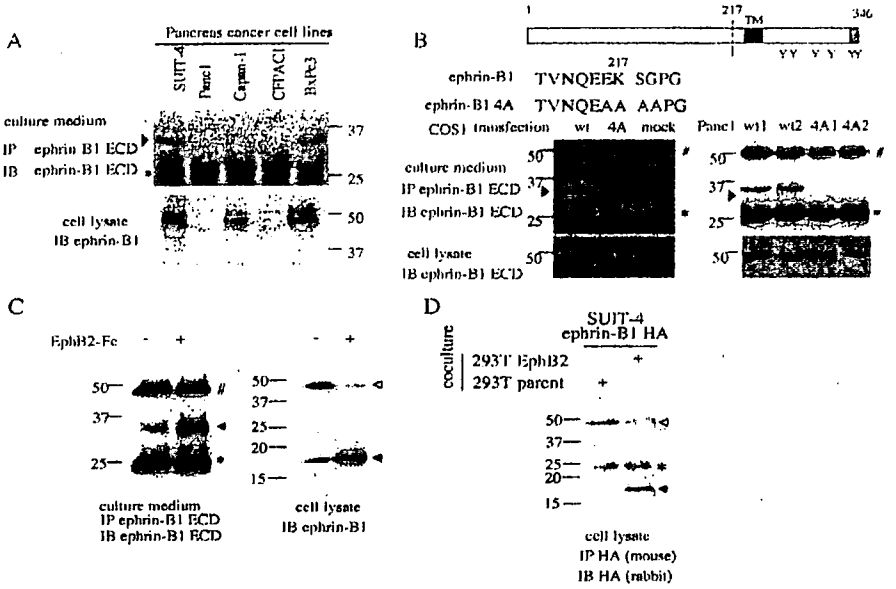

Fig. 1. The ectodomain of ephrin-B1 is secreted into the culture medium of human pancreas cancer cells. (A) Various pancreas cancer cell lines were cultured in medium containing 0.5% FBS. After 6 hours, conditioned medium was collected and subjected to immunoprecipitation (IP) and immunoblotting (IB) with polyclonal antibodies against the extracellular domain of ephrin-B1 (ephrin-B1 ECD). The immunoprecipitated 35 kDa ephrin-B1 fragment is indicated by an arrowhead. The expression of ephrin-B1 in each cell lysate was confirmed by immunoblotting (bottom). (B) A diagram of ephrin-B1 is shown at the top. TM, transmembrane domain; Y, tyrosine phosphorylation sites. Dotted line indicates the cleavage site of ephrin-B1, and the PDZ domain-binding motif is indicated as a gray box at the C-terminus. Four aa residues around the cleavage site were changed to alanine (ephrin-B1 4A) destroying the MMP-8 cleavage site. The conditioned medium of COS-1 cells transfected with wild-type (wt) or mutant ephrin-B1 (4A), or independent PANC-1 clones stably expressing ephrin-B1 were collected and subjected to immunoprecipitation and immunoblotting as described in A. (C) SUIT-4 cells were either treated with EphB2-Fc (4 μg/ml) for 2 hours (+) or left untreated (–). The ephrin-B1 fragment in the medium was detected as in A (left) or the cell lysates were subjected to immunoblotting with anti ephrin-B1 C18 (right panel). Open and filled arrowheads indicate uncleaved ephrin-B1 and its processed fragment (p17), respectively. (D) SUIT-4 cells were transiently transfected with ephrin-B1 tagged with HA at the C-terminus. Transfected SUIT-4 cells were overlayed on a monolayer of parent HEK293T cells or HEK293T cells stably expressing EphB2 for 2 hours. Cell lysates were prepared from co-cultured cells to detect HA-tagged p17 fragment derived from exogenously expressed ephrin-B1 in SUIT-4 cells by immunoprecipitation. # and * indicate the IgG heavy chain and light chain, respectively. Open and filled arrowheads indicate uncleaved ephrin-B1 and its processed fragment (p17), respectively.

induced by stimulation of ephrin-B1 did not depend on the elevation of MMP-8 expression level, but rather it was suggested to depend on the intracellular signaling mediated by ephrin-B1.

MMP-8, also known as neutrophil collagenase, is not only expressed in neutrophils, but it is also expressed in wide variety of cells, including chondrocytes, endothelial cells, synovial fibroblast and various cancer cells (Siller-Lopez et al., 2000; Stadlemann et al., 2003; Lint and Libert, 2006). MMP-8 cleaves all three α-chains of type I, II and III collagen and also a wide range of non-collagenous substrates, and plays important roles in inflammation and in cancer progression (Lint and Libert, 2006). Like other secretory proteins, proenzymes of soluble-type MMPs are secreted after the process of vesicle transport from Golgi to the plasma membrane, and then, extracellularly activated by removal of the propeptide domain (Sternlicht and Werb, 2001). In neutrophils, MMP-8 is stored in specific granules after being transported from Golgi, and released following activation by inflammatory mediators (Sternlicht and Werb, 2001), however, whether it is also the case in various cancer cells has yet to be fully investigated. Our analysis of the interaction between MMP-8 activity and EphB-ephrin-B1 signal transduction revealed a novel function of the C-terminus of ephrin-B1 in the secretion of MMP-8, which leads to the cleavage of ephrin-B1 and involves the negative regulation of the EphB-ephrin-B1 complex. Moreover, regulation of this MMP family member through the ephrin-B1 C-terminus may contribute to the highly invasive phenotype of ephrin-B1-expressing cancer cells by degradation of the extracellular matrix.

Results

The Ephrin-B1 ectodomain is secreted into the culture medium of pancreatic cancer cell lines

During screening of peptides secreted by the pancreatic cancer cell line SUIT-4, we identified,using MALDI-MS/MS analysis, three different peptides derived from ephrin-B1 sharing a common N-terminus. Analysis of these peptides indicated that ephrin-B1 undergoes limited cleavage between aa residues 217 and 218. Immunoprecipitation with antibodies against the extracellular domain of ephrin-B1 revealed a 35 kDa band from the conditioned media of two out of five pancreatic cancer cell lines. The 35 kDa fragment was also detected in COS-1 and PANC-1 cells when ephrin-B1 was expressed (Fig. 1A,B). These results indicate that the 35 kDa ectodomain fragment is released by cleavage of ephrin-B1 in these cell lines. The concentration of serum in the medium did not affect the cleavage of ephrin-B1 (data not shown). The cleavage site in ephrin-B1 estimated by MALDI-MS/MS was confirmed by the observation that substitution of the four amino acids (aa) at positions 216-219 (ephrin-B1$^{216\text{-}219}$) by alanine (ephrin-B1 4A), blocked the production of the 35 kDa ectodomain fragment in COS-1 and PANC-1 cells (Fig. 1B).

Cleavage of ephrin-B1 ectodomain is enhanced by interaction with its receptor EphB2, which is regulated by the C-terminus of ephrin-B1

Next, we examined whether the interaction of ephrin-B1 with its receptor EphB2 modifies the cleavage of ephrin-B1.

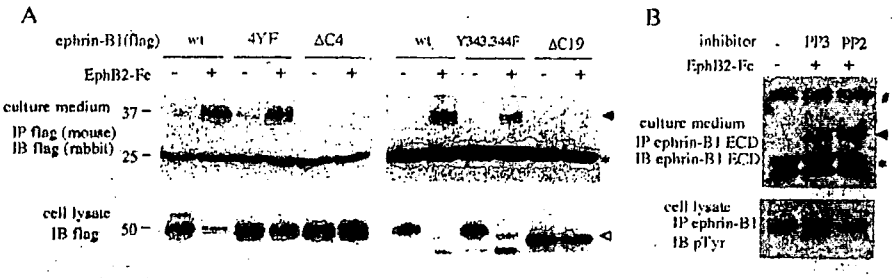

Fig. 2. Activation of ephrin-B1 cleavage requires its C-terminus. (A) Wild-type and various mutants of ephrin-B1 tagged with Flag at the N-terminus were expressed in Capan-1 cells by retrovirus-mediated gene transfer. The cells were treated with EphB2-Fc (2 μg/ml) for 1.5 hours (+) or left untreated (–) and conditioned medium was assayed for the presence of ephrin-B1 fragments by immunoprecipitation (IP) and immunoblotting (IB) with anti-flag antibody. The filled arrowhead indicates the ephrin-B1 ectodomain fragment. (Bottom) Expression of wild-type or mutated ephrin-B1 in cell lysates after treatment with EphB2-Fc. The open arrowhead indicates ephrin-B1 ΔC19. (B) SUIT-4 cells were treated with EphB2-Fc and PP2 or control PP3or left untreated, as indicated. Conditioned medium was collected after 2 hours and subjected to immunoprecipitation and immunoblotting. In the bottom panel, suppression of tyrosine phosphorylation of ephrin-B1 by PP2 treatment is shown. # and * indicate the IgG heavy chain and light chain, respectively.

Incubation of SUIT-4 cells with purified EphB2-Fc, a fusion protein of the extracellular domain of EphB2 with the Fc fragment of mouse IgG2b, significantly increased the amount of the 35 kDa fragment of ephrin-B1 in the conditioned medium (Fig. 1C, left). In EphB2-Fc-treated cell extract, a cellular fragment of ephrin-B1, produced by ectodomain shedding, was detected by immunoblotting with an antibody reacting to the C-terminal of ephrin-B1, as a band at 17 kDa (p17; Fig. 1C, right). The accumulation of p17 was also detected in ephrin-B1-expressing cells after contact with cells expressing EphB2. When ephrin-B1-expressing cells were overlayed on EphB2-expressing cells and co-cultured, significant reduction of uncleaved ephrin-B1 together with production of the p17 fragment was observed (Fig. 1D). This result indicates that cleavage of ephrin-B1 is also enhanced when ephrin-B1-expressing cells contact with heterologous cells expressing the EphB2.

In order to examine the processing mechanism of the ephrin-B1 ectodomain, several mutants of ephrin-B1 were analyzed. The cleavage of ephrin-B1 was also increased by EphB2-Fc treatment of Capan-1 cells expressing wild-type ephrin-B1 (Fig. 2A). However, expression of ephrin-B1 lacking the C-terminus (ΔC4 and ΔC19; the MMP-8 cleavage site at aa 217-218 is intact in these mutants), did not produce the 35 kDa ectodomain fragment in the culture medium upon treatment with EphB2-Fc (Fig. 2A). However, mutation of any of the four tyrosine residues in the cytoplasmic region (4YF) and tyrosines located at the C-terminus of ephrin-B1 (Y343, 344F) did not affect ephrin-B1 cleavage (Fig. 2A). In contrast to the significant reduction of full length wild-type or YF mutants of ephrin-B1 in cell lysates after EphB2-Fc treatment, level of C-terminally truncated ephrin-B1 mutants remained almost unchanged (Fig. 2A, bottom panels). We also observed similar results using PANC-1 cells, and confirmed that expression of ΔC mutants were localized on cell membrane (data not shown). In addition, treatment with PP2, an inhibitor of Src family kinases, significantly blocked tyrosine phosphorylation of ephrin-B1, but it did not affect cleavage of ephrin-B1 (Fig. 2B). Thus, the C-terminus of ephrin-B1, but not tyrosine phosphorylation of ephrin-B1, is required for induction of the proteolysis of ephrin-B1.

The Ephrin-B1 ectodomain is processed by MMP-8

The cleavage of ephrin-B1 was inhibited in PANC-1 cells expressing ephrin-B1, by incubation with the pan-matrix metalloproteinase (MMP) inhibitor GM6001, but not by inhibitors of other proteases including a cysteine protease, a serine protease, an aspartic protease or calpain (Fig. 3A). The amount of cleaved ephrin-B1 ectodomain was increased by treatment of DCI (3,4-dichloroisocoumarin), a serine protease inhibitor and TPCK (N^{α}-tosyl-phe chloromethyl ketone), a chymotrypsin inhibitor of unknown function. As the inhibition of ephrin-B1 cleavage by GM6001 was also confirmed in SUIT-4 cells (data not shown), we further attempted to identify the metalloproteinase responsible. When SUIT-4 cells were treated with natural MMP inhibitors, TIMPs, at low concentration (100 nM), cleavage of ephrin-B1 was most effectively inhibited by TIMP-1 compared with TIMP-2 and TIMP-3 (Fig. 3B). TIMP-3, which is known to inhibit tumor necrosis factor-α converting enzyme (TACE) did not inhibit the cleavage of ephrin-B1 at all at concentrations from 5-250 nM (data not shown), whereas it completely inhibited the cleavage of TNF-α expressed in THP-1 cells at 100 nM (Fig. 3B, right panel). Among inhibitors of several MMPs expressed in SUIT-4 cells, including MMP-1, MMP-2 or 3, MMP-8 and MMP-9, only the inhibitor of MMP-8 blocked the cleavage of ephrin-B1 (Fig. 3C), and this effect was also seen in COS-1 cells and PANC-1 cells expressing ephrin-B1 (data not shown).

In order to examine whether MMP-8 cleaves ephrin-B1, ephrin-B1-Fc fusion protein, which consists of the entire extracellular region of ephrin-B1 and the Fc fragment of mouse IgG2b, was incubated with purified activated MMPs in vitro. Incubation of ephrin-B1-Fc with activated MMP-8 produced two fragments of ephrin-B1-Fc corresponding to the predicted sizes (Fig. 3D). However, other membrane-type metalloproteinases such as MT1-MMP and ADAM10, which are also expressed in SUIT-4 cells, did not cleave ephrin-B1-Fc in vitro (Fig. 3D).

Expression of MMP-8 protein was detected at approximately the same levels in all of the cell lines we examined (Fig. 4A, left), although it was detected at high level when the cells were replated and decreased after the cells reached confluence (Fig. 4A, right). When expression of

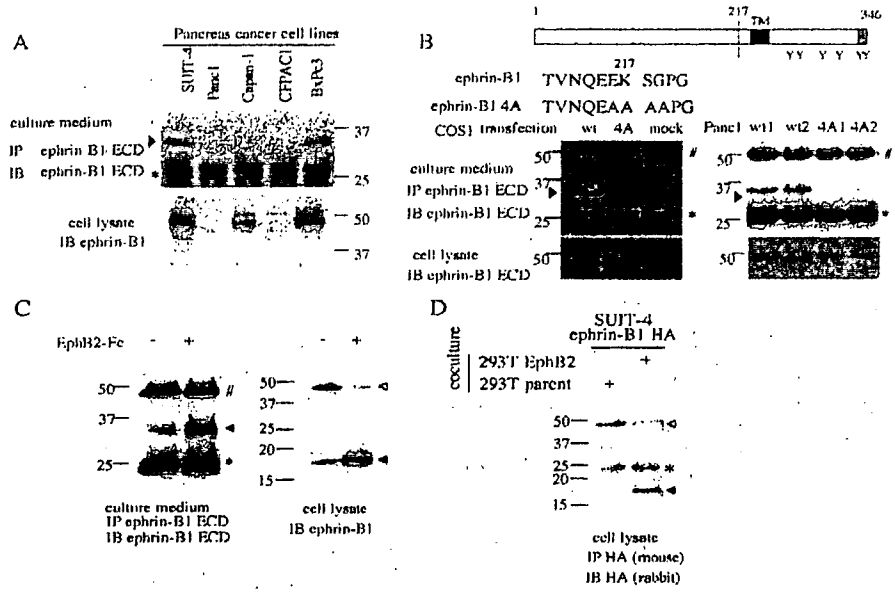

Fig. 1. The ectodomain of ephrin-B1 is secreted into the culture medium of human pancreas cancer cells. (A) Various pancreas cancer cell lines were cultured in medium containing 0.5% FBS. After 6 hours, conditioned medium was collected and subjected to immunoprecipitation (IP) and immunoblotting (IB) with polyclonal antibodies against the extracellular domain of ephrin-B1 (ephrin-B1 ECD). The immunoprecipitated 35 kDa ephrin-B1 fragment is indicated by an arrowhead. The expression of ephrin-B1 in each cell lysate was confirmed by immunoblotting (bottom). (B) A diagram of ephrin-B1 is shown at the top. TM, transmembrane domain; Y, tyrosine phosphorylation sites. Dotted line indicates the cleavage site of ephrin-B1, and the PDZ domain-binding motif is indicated as a gray box at the C-terminus. Four aa residues around the cleavage site were changed to alanine (ephrin-B1 4A) destroying the MMP-8 cleavage site. The conditioned medium of COS-1 cells transfected with wild-type (wt) or mutant ephrin-B1 (4A), or independent PANC-1 clones stably expressing ephrin-B1 were collected and subjected to immunoprecipitation and immunoblotting as described in A. (C) SUIT-4 cells were either treated with EphB2-Fc (4 μg/ml) for 2 hours (+) or left untreated (–). The ephrin-B1 fragment in the medium was detected as in A (left) or the cell lysates were subjected to immunoblotting with anti ephrin-B1 C18 (right panel). Open and filled arrowheads indicate uncleaved ephrin-B1 and its processed fragment (p17), respectively. (D) SUIT-4 cells were transiently transfected with ephrin-B1 tagged with HA at the C-terminus. Transfected SUIT-4 cells were overlayed on a monolayer of parent HEK293T cells or HEK293T cells stably expressing EphB2 for 2 hours. Cell lysates were prepared from co-cultured cells to detect HA-tagged p17 fragment derived from exogenously expressed ephrin-B1 in SUIT-4 cells by immunoprecipitation. # and * indicate the IgG heavy chain and light chain, respectively. Open and filled arrowheads indicate uncleaved ephrin-B1 and its processed fragment (p17), respectively.

induced by stimulation of ephrin-B1 did not depend on the elevation of MMP-8 expression level, but rather it was suggested to depend on the intracellular signaling mediated by ephrin-B1.

MMP-8, also known as neutrophil collagenase, is not only expressed in neutrophils, but it is also expressed in wide variety of cells, including chondrocytes, endothelial cells, synovial fibroblast and various cancer cells (Siller-Lopez et al., 2000; Stadlemann et al., 2003; Lint and Libert, 2006). MMP-8 cleaves all three α-chains of type I, II and III collagen and also a wide range of non-collagenous substrates, and plays important roles in inflammation and in cancer progression (Lint and Libert, 2006). Like other secretory proteins, proenzymes of soluble-type MMPs are secreted after the process of vesicle transport from Golgi to the plasma membrane, and then, extracellularly activated by removal of the propeptide domain (Sternlicht and Werb, 2001). In neutrophils, MMP-8 is stored in specific granules after being transported from Golgi, and released following activation by inflammatory mediators (Sternlicht and Werb, 2001), however, whether it is also the case in various cancer cells has yet to be fully investigated. Our analysis of the interaction between MMP-8 activity and EphB-ephrin-B1 signal transduction revealed a novel function of the C-terminus of ephrin-B1 in the secretion of MMP-8, which leads to the cleavage of ephrin-B1 and involves the negative regulation of the EphB-ephrin-B1 complex. Moreover, regulation of this MMP family member through the ephrin-B1 C-terminus may contribute to the highly invasive phenotype of ephrin-B1-expressing cancer cells by degradation of the extracellular matrix.

Results

The Ephrin-B1 ectodomain is secreted into the culture medium of pancreatic cancer cell lines

During screening of peptides secreted by the pancreatic cancer cell line SUIT-4, we identified,using MALDI-MS/MS analysis, three different peptides derived from ephrin-B1 sharing a common N-terminus. Analysis of these peptides indicated that ephrin-B1 undergoes limited cleavage between aa residues 217 and 218. Immunoprecipitation with antibodies against the extracellular domain of ephrin-B1 revealed a 35 kDa band from the conditioned media of two out of five pancreatic cancer cell lines. The 35 kDa fragment was also detected in COS-1 and PANC-1 cells when ephrin-B1 was expressed (Fig. 1A,B). These results indicate that the 35 kDa ectodomain fragment is released by cleavage of ephrin-B1 in these cell lines. The concentration of serum in the medium did not affect the cleavage of ephrin-B1 (data not shown). The cleavage site in ephrin-B1 estimated by MALDI-MS/MS was confirmed by the observation that substitution of the four amino acids (aa) at positions 216-219 (ephrin-B1$^{216\text{-}219}$) by alanine (ephrin-B1 4A), blocked the production of the 35 kDa ectodomain fragment in COS-1 and PANC-1 cells (Fig. 1B).

Cleavage of ephrin-B1 ectodomain is enhanced by interaction with its receptor EphB2, which is regulated by the C-terminus of ephrin-B1

Next, we examined whether the interaction of ephrin-B1 with its receptor EphB2 modifies the cleavage of ephrin-B1.

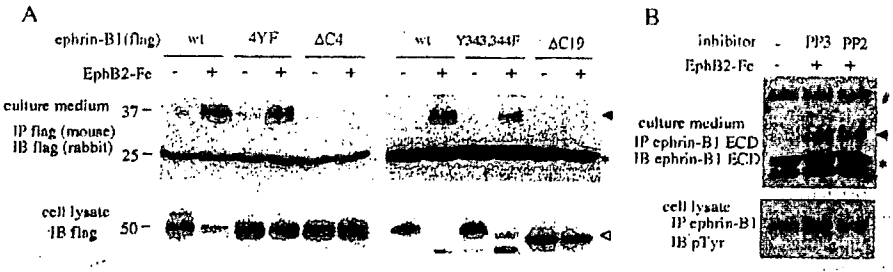

Fig. 2. Activation of ephrin-B1 cleavage requires its C-terminus. (A) Wild-type and various mutants of ephrin-B1 tagged with Flag at the N-terminus were expressed in Capan-1 cells by retrovirus-mediated gene transfer. The cells were treated with EphB2-Fc (2 μg/ml) for 1.5 hours (+) or left untreated (–) and conditioned medium was assayed for the presence of ephrin-B1 fragments by immunoprecipitation (IP) and immunoblotting (IB) with anti-flag antibody. The filled arrowhead indicates the ephrin-B1 ectodomain fragment. (Bottom) Expression of wild-type or mutated ephrin-B1 in cell lysates after treatment with EphB2-Fc. The open arrowhead indicates ephrin-B1 ΔC19. (B) SUIT-4 cells were treated with EphB2-Fc and PP2 or control PP3or left untreated, as indicated. Conditioned medium was collected after 2 hours and subjected to immunoprecipitation and immunoblotting. In the bottom panel, suppression of tyrosine phosphorylation of ephrin-B1 by PP2 treatment is shown. # and * indicate the IgG heavy chain and light chain, respectively.

Incubation of SUIT-4 cells with purified EphB2-Fc, a fusion protein of the extracellular domain of EphB2 with the Fc fragment of mouse IgG2b, significantly increased the amount of the 35 kDa fragment of ephrin-B1 in the conditioned medium (Fig. 1C, left). In EphB2-Fc-treated cell extract, a cellular fragment of ephrin-B1, produced by ectodomain shedding, was detected by immunoblotting with an antibody reacting to the C-terminal of ephrin-B1, as a band at 17 kDa (p17; Fig. 1C, right). The accumulation of p17 was also detected in ephrin-B1-expressing cells after contact with cells expressing EphB2. When ephrin-B1-expressing cells were overlayed on EphB2-expressing cells and co-cultured, significant reduction of uncleaved ephrin-B1 together with production of the p17 fragment was observed (Fig. 1D). This result indicates that cleavage of ephrin-B1 is also enhanced when ephrin-B1-expressing cells contact with heterologous cells expressing the EphB2.

In order to examine the processing mechanism of the ephrin-B1 ectodomain, several mutants of ephrin-B1 were analyzed. The cleavage of ephrin-B1 was also increased by EphB2-Fc treatment of Capan-1 cells expressing wild-type ephrin-B1 (Fig. 2A). However, expression of ephrin-B1 lacking the C-terminus (ΔC4 and ΔC19; the MMP-8 cleavage site at aa 217-218 is intact in these mutants), did not produce the 35 kDa ectodomain fragment in the culture medium upon treatment with EphB2-Fc (Fig. 2A). However, mutation of any of the four tyrosine residues in the cytoplasmic region (4YF) and tyrosines located at the C-terminus of ephrin-B1 (Y343, 344F) did not affect ephrin-B1 cleavage (Fig. 2A). In contrast to the significant reduction of full length wild-type or YF mutants of ephrin-B1 in cell lysates after EphB2-Fc treatment, level of C-terminally truncated ephrin-B1 mutants remained almost unchanged (Fig. 2A, bottom panels). We also observed similar results using PANC-1 cells, and confirmed that expression of ΔC mutants were localized on cell membrane (data not shown). In addition, treatment with PP2, an inhibitor of Src family kinases, significantly blocked tyrosine phosphorylation of ephrin-B1, but it did not affect cleavage of ephrin-B1 (Fig. 2B). Thus, the C-terminus of ephrin-B1, but not tyrosine phosphorylation of ephrin-B1, is required for induction of the proteolysis of ephrin-B1.

The Ephrin-B1 ectodomain is processed by MMP-8

The cleavage of ephrin-B1 was inhibited in PANC-1 cells expressing ephrin-B1, by incubation with the pan-matrix metalloproteinase (MMP) inhibitor GM6001, but not by inhibitors of other proteases including a cysteine protease, a serine protease, an aspartic protease or calpain (Fig. 3A). The amount of cleaved ephrin-B1 ectodomain was increased by treatment of DCI (3,4-dichloroisocoumarin), a serine protease inhibitor and TPCK (N^{α}-tosyl-phe chloromethyl ketone), a chymotrypsin inhibitor of unknown function. As the inhibition of ephrin-B1 cleavage by GM6001 was also confirmed in SUIT-4 cells (data not shown), we further attempted to identify the metalloproteinase responsible. When SUIT-4 cells were treated with natural MMP inhibitors, TIMPs, at low concentration (100 nM), cleavage of ephrin-B1 was most effectively inhibited by TIMP-1 compared with TIMP-2 and TIMP-3 (Fig. 3B). TIMP-3, which is known to inhibit tumor necrosis factor-α converting enzyme (TACE) did not inhibit the cleavage of ephrin-B1 at all at concentrations from 5-250 nM (data not shown), whereas it completely inhibited the cleavage of TNF-α expressed in THP-1 cells at 100 nM (Fig. 3B, right panel). Among inhibitors of several MMPs expressed in SUIT-4 cells, including MMP-1, MMP-2 or 3, MMP-8 and MMP-9, only the inhibitor of MMP-8 blocked the cleavage of ephrin-B1 (Fig. 3C), and this effect was also seen in COS-1 cells and PANC-1 cells expressing ephrin-B1 (data not shown).

In order to examine whether MMP-8 cleaves ephrin-B1, ephrin-B1-Fc fusion protein, which consists of the entire extracellular region of ephrin-B1 and the Fc fragment of mouse IgG2b, was incubated with purified activated MMPs in vitro. Incubation of ephrin-B1-Fc with activated MMP-8 produced two fragments of ephrin-B1-Fc corresponding to the predicted sizes (Fig. 3D). However, other membrane-type metalloproteinases such as MT1-MMP and ADAM10, which are also expressed in SUIT-4 cells, did not cleave ephrin-B1-Fc in vitro (Fig. 3D).

Expression of MMP-8 protein was detected at approximately the same levels in all of the cell lines we examined (Fig. 4A, left), although it was detected at high level when the cells were replated and decreased after the cells reached confluence (Fig. 4A, right). When expression of

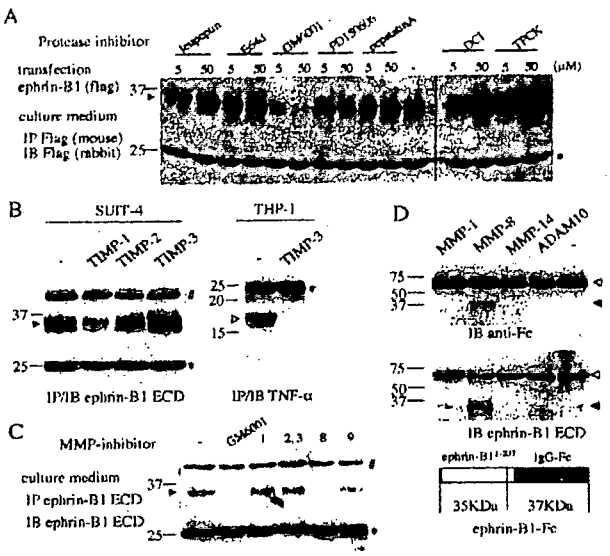

Fig. 3. Screening of a protease that cleaves the extracellular domain of ephrin-B1. (A) Panc-1 cells transiently expressing Flag-tagged ephrin-B1 were incubated with various protease inhibitors for 4 hours in medium containing 0.5% FBS: leupeptin and E64d (Loxistatin), a cystein protease inhibitor; GM6001, a pan-MMP inhibitor; PD150606, a calpain inhibitor; pepstatin A, an aspartic protease inhibitor; DCI (3,4-dichloroisocoumarin), a serine protease inhibitor; TPCK (N$^{\alpha}$-tosyl-phe chloromethyl ketone), a chymotrypsin inhibitor. The cleavage of ephrin-B1 ectodomain was examined as described in Fig. 2A. (B) Left: SUIT-4 cells were incubated with EphB2-Fc (2 μg/ml) together with or without TIMPs (100 nM for each) as indicated for 2 hours. The processed ephrin-B1 fragment was detected in the culture medium. Right: THP-1 cells were treated with PMA (10 ng/ml) together with or without TIMP-3 (100 nM) for 6 hours. Open arrowhead indicates the processed fragment of TNF-α in the medium detected by immunoprecipitation with anti TNF-α antibody. (C) SUIT-4 cells were treated with various MMP inhibitors as indicated (1 μM for MMP-8 inhibitor and 5 μM for others) for 4 hours. Ephrin-B1 fragment was detected in the medium. (D) Purified ephrin-B1-Fc protein was incubated with activated MMP in vitro for 1 hour at 37°C, separated by SDS-PAGE, and immunoblotted with anti-Fc mouse IgG or anti-ephrin-B1. Bottom: a schematic representation of ephrin-B1-Fc with the MMP-8 cleavage site indicated by a dotted line. Open and filled arrowheads indicate uncleaved ephrin-B1-Fc and the processed fragments, respectively.

MMP-8 was reduced in SUIT-4 cells by treatment of cells with siRNA, the amount of processed ephrin-B1 ectodomain in the culture medium was decreased (Fig. 4B). By contrast, overexpression of activated MMP-8 cDNA, in which the propeptide domain was removed, in SUIT-4 cells evidently increased the cleavage of ephrin-B1 (Fig. 4C).

As some MMPs and their substrates physically associate directly or indirectly and make a protein complex, interaction between MMP-8 and ephrin-B1 was examined (Sawicki et al., 2005; Yu et al., 2007). Ephrin-B1 was coprecipitated with MMP-8 from extracts of L ephrin-B1 cells by MMP-8-specific antibodies, but not by control normal rabbit IgG1, indicating that MMP-8 forms a complex with ephrin-B1 (Fig. 4D). However, association of MMP-8 with the receptor EphB2 was not detected (data not shown). These results also suggest that MMP-8 is the key metalloproteinase that cleaves the ephrin-B1 ectodomain.

Stimulation of ephrin-B1 activates secretion of MMP-8, which is regulated by the C-terminus of ephrin-B1

To understand the mechanism of activation of ephrin-B1 cleavage by EphB2, we next examined whether it is accompanied by an increase in MMP-8 expression. The level of intracellular expression of MMP-8 mRNA was not affected by treatment with EphB2-Fc or contact of ephrin-B1-expressing cells with EphB2-expressing cells for 4 hours or longer (Fig. 5A). Moreover, the amount of processed ephrin-B1 ectodomain produced in the medium was not altered by the addition of cyclohexamide or actinomysin D, inhibitors of de novo synthesis of mRNA and proteins, respectively (Fig. 5B). These results indicate that activation of ephrin-B1 cleavage by EphB2 does not depend on the increased amount of MMP-8. In addition, when the de novo synthesis of MMP-8 was blocked, the amount of intracellular MMP-8 protein decreased slightly after 4 hours or longer treatment of ephrin-B1-expressing cells with EphB2-Fc (Fig. 5C), which suggests that stimulation of ephrin-B1 activates extracellular release of MMP-8 protein from the cytoplasm. Actually, the amount of MMP-8 protein in the culture medium was remarkably elevated after incubation of the cells with EphB2-Fc as detected by immunoprecipitation (Fig. 5D).

In order to show directly that stimulation of ephrin-B1 increased exocytosis of MMP-8, which was already synthesized and present in the cytoplasm, SUIT-4 cells were pulse-labeled with [^{35}S]methionine. When pulse-labeled cells were treated with EphB2-Fc, a higher amount of labeled MMP-8 protein was detected in the medium compared to treatment of cells with Fc (Fig. 5E, left). However, secretion of labeled MMP-7, which was examined as a control, was not altered by EphB2-Fc treatment (Fig. 5E, right). In addition, the secretion of [^{35}S]methionine-labeled MMP-8 was also increased by EphB2-Fc treatment of Capan-1 cells expressing wild-type ephrin-B1, but it was not found in the media of cells expressing ephrin-B1 lacking the C-terminus (ΔC4 and ΔC19) (Fig. 5F, left). Consistently, the total amount of MMP-8 protein in the culture medium from cells expressing wild-type ephrin-B1 was higher than in the medium from ΔC4 ephrin-B1-expressing cells (Fig. 5F, right). These results suggest that stimulation of ephrin-B1 by EphB2 upregulates the process of MMP-8 exocytosis, and the C-terminus of ephrin-B1 regulates this event.

Stimulation of ephrin-B1 by EphB2 induces activation of Arf1 GTPase

To further confirm that activation of MMP-8 secretion is involved in the elevated ephrin-B1 cleavage in response to stimulation with EphB2, the cells were treated with brefeldin A, an inhibitor of membrane trafficking through the Golgi, which blocks the secretion of proteins (Tamaki and Yamashina, 2002). EphB2-stimulated cleavage of ephrin-B1 was apparently reduced by brefeldin A treatment (Fig. 6A). As a mode of action of brefeldin A is to inhibit activation of ADP ribosylation factor 1 (Arf1), a ras family GTPase, by blocking of the exchange reaction from Arf1-GDP to Arf1-GTP (Niu et al., 2005; Zeeh et al., 2006), we further examined the activity of Arf1 in ephrin-

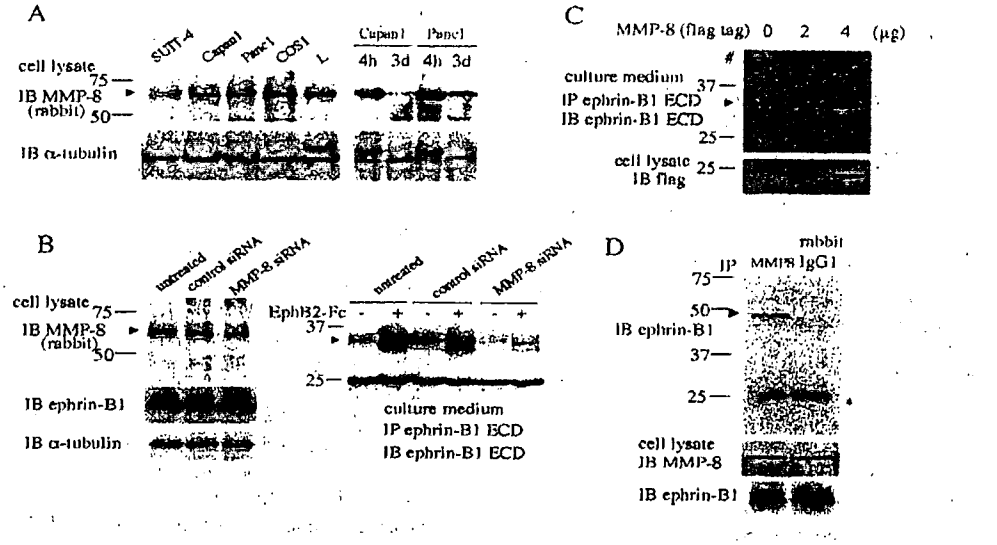

Fig. 4. MMP-8 is the key protease of ephrin-B1 cleavage. (A) Expression of MMP-8 in cell lysates. Left: The indicated cells were seeded on plates not to reach confluence. Cell lysates were prepared on the day after plating. Right: cell lysates were prepared 4 hours (4h) or 3 days (d3) after being plated on dishes. The cells were confluent on day 3 after plating. (B) SUIT-4 cells treated with either MMP-8 siRNA or control scrambled siRNA (control), or left untreated. The cells were detached 48 hours later, replated on new plates and further incubated for 24 hours. Left: Cellular levels of MMP-8 were analyzed 72 hours after treatment of SUIT-4 cells with siRNAs. Right: the culture medium was replaced with one fresh medium or medium containing EphB2-Fc (2 g/ml) and incubated for 2 hours to detect ephrin-B1 ectodomain in the medium. (C) SUIT-4 cells were transiently transfected with the indicated volume of a plasmid encoding Flag-tagged activated MMP-8 cDNA. After 48 hours of transfection, the medium was replaced and the cells were further incubated for 6 hours to detect processed ephrin-B1 ectodomain in the medium. The expression of transfected MMP-8 in each cell lysate was confirmed by immunoblotting with anti-Flag antibody (bottom). (D) The lysate of L ephrin-B1 cells was immunoprecipitated with anti-MMP-8 polyclonal antibody or control rabbit IgG1, and subjected to immunoblotting with anti-ephrin-B1 C18 antibody. HRP-conjugated anti-rabbit IgG (TrueBlot) was used as the secondary antibody for immunoblotting to avoid cross reaction with denatured rabbit IgG heavy chain of the antibody used for immunoprecipitation. The arrowhead indicates coprecipitated ephrin-B1. The asterisk indicates the IgG light chain.

B1-expressing cancer cells. To examine the amount of activated, GTP-bound Arf1, a pull-down approach was performed with an adaptor protein GGA3, which specifically binds to GTP-bound Arfs (Dell'Angelica et al., 2000). As a control experiment, we confirmed that constitutively activated Arf1 (Q71L), but not a dominant negative mutant of Arf1 (T31N) was coprecipitated with GST-tagged GGA3 (Fig. 6B, right panel). Incubation of SUIT-4 cells with EphB2-Fc increased the amount of Arf1-GTP coprecipitated with GST-tagged GGA3 (Fig. 6B). Similar results were also observed in PANC-1 cells expressing ephrin-B1, whereas treatment with EphB2-Fc did not affect activation of Arf1 in parent PANC-1 cells, which express ephrin-B1 in trace amounts (Fig. 6B). The amount of Arf1-GTP was also increased by EphB2-Fc treatment of Capan-1 cells expressing wild-type ephrin-B1 or ephrin-B1 4YF mutant, but not in cells expressing ΔC4 ephrin-B1 (Fig. 6C). These results suggest that stimulation of ephrin-B1 by EphB2 activates Arf1, and the signaling mediated by the C-terminus of ephrin-B1 is involved in this pathway. Furthermore, treatment of cells with brefeldin A, or overexpression of dominant negative mutant of Arf1, Arf1 T31N, decreased the secretion of MMP-8 in Capan-1 cells, indicating that Arf1 regulates the secretion of MMP-8 (Fig. 6D).

The C-terminus of ephrin-B1 is involved in the invasion by cancer cells

To investigate the biological implication of metalloproteinase activation caused by ephrin-B1-mediated signaling, we examined changes in the invasiveness of ephrin-B1-expressing cells with or without stimulation by EphB2 using an in vitro cell invasion assay. The invasion of collagen by Capan-1 cells was promoted by expression of ephrin-B1 and treatment of the cells with EphB2-Fc, and this invasion was inhibited by the addition of an MMP-8 inhibitor (Fig. 7A). On the other hand, the invasion by Capan-1 cells expressing ΔC4 ephrin-B1, or by parent Capan-1 cells was not significantly promoted by EphB2-Fc treatment (Fig. 7A).

We further examined whether expression of ephrin-B1 actually promotes cancer cell invasion in vivo using PANC-1 cells as a model system to study peritoneal dissemination. PANC-1 cells stably expressing wild-type ephrin-B1 (PANC-1 ephrin-B1) or ΔC4 ephrin-B1 (PANC-1 ΔC4) were established to compare their invasiveness with that of parent PANC-1 cells. Expression of wild-type or mutated ephrin-B1 did not affect BrdU incorporation into cells grown under normal two-dimensional cell culture conditions (data not shown). When these cells were injected intraperitoneally into nude mice, PANC-1 ephrin-B1 cells formed many tumor nodules in the mesenteric sheets and also in the peritoneal cavity, including the rectouterine region. By contrast, in mice injected with parent PANC-1 cells or PANC-1 ΔC4 cells, such tumors in mesentery sheets were fewer and smaller, and the total tumor volume involving the rectouterine region was much less (Fig. 7B,C, Table 1). The cells composing the mesenteric sheets express cognate receptors for ephrin-B1, EphB2 and

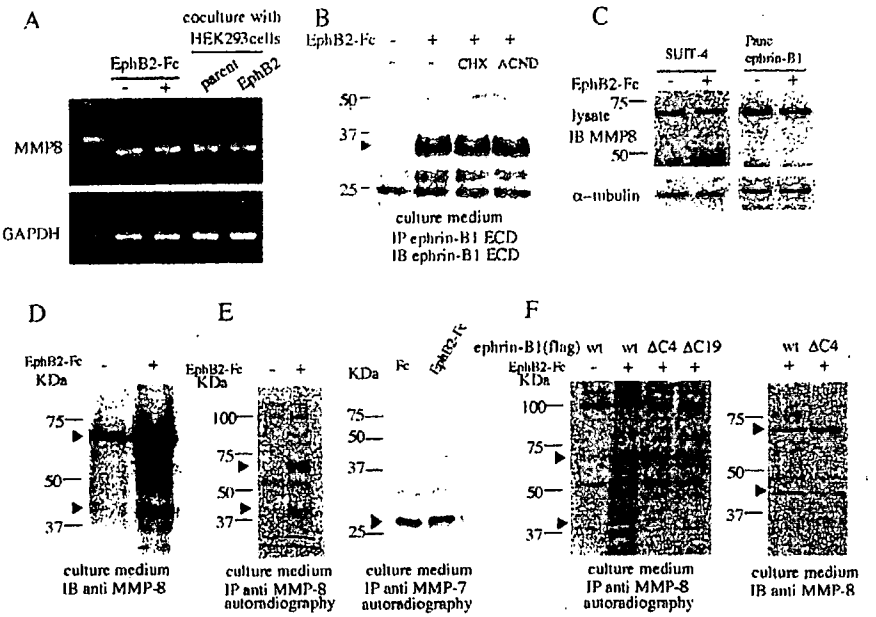

Fig. 5. Stimulation of ephrin-B1 with EphB2 increases MMP-8 secretion. (A) SUIT-4 cells were left untreated or were treated with EphB2-Fc or co-cultured with either parent or EphB2-expressing HEK293 cells for 4 hours. Cellular levels of MMP-8 were analyzed by RT-PCR using GAPDH as a control. (B) SUIT-4 cells were incubated with or without EphB2-Fc for 2 hours in the presence or absence of cyclohexamide (CHX, 100 μg/ml) or actinomycin D (ACND, 5 μg/ml) to detect the ephrin-B1 ectodomain in the medium. (C) SUIT-4 cells or PANC-1 cells stably expressing ephrin-B1 were treated with actinomycin D (5 μg/ml) together with or without EphB2-Fc (2 μg/ml) for 4 hours. Cell lysates were prepared and intracellular expression levels of MMP-8 were analyzed by western blotting using α-tubulin as a loading control. (D) Conditioned medium of SUIT-4 cells were collected after the cells were treated with EphB2-Fc or left untreated for 4 hours in serum-free medium. Proteins secreted in the medium were precipitated with trichloroacetic acid (10%), resuspended in sample buffer, and subjected to immunoblotting with anti MMP-8 polyclonal antibody. Arrowheads indicate MMP-8 protein (proenzyme and activated). (E) SUIT-4 cells were metabolically labeled with [^{35}S]methionine, then treated with EphB2-Fc or control Fc for 2 hours. The amount of labeled MMP-8 (left panel) or MMP-7 (right panel) in the medium was evaluated through immunoprecipitation from the conditioned medium followed by SDS-PAGE and autoradiography. Arrowhead indicates MMP-8 (proenzyme and activated; left) or MMP-7 (right) in the medium. (F) Wild-type and mutants of ephrin-B1 were expressed in Capan-1 cells as in Fig. 2A, and [^{35}S]methionine-labeled MMP-8 was detected in the medium (left panel). Right: The total amount of MMP-8 in the conditioned medium of Capan-1 cells was evaluated using the trichloroacetic acid (TCA) precipitation procedure, followed by immunoblotting with anti MMP-8 antibody as in D.

EphB4 (see Fig. S1 in supplementary material). These results indicate that ephrin-B1 actually promotes cancer cell invasion, which requires the C-terminus of ephrin-B1. EphB2 and EphB4 expressed in cells of the mesenteric sheet might act as interaction partners for ephrin-B1 present on PANC-1 cells.

Discussion

The interaction of Eph family receptor protein tyrosine kinases with their ligands, ephrin family proteins, induces bi-directional signaling. In this study, we showed for the first time that ephrin-B1 regulates the activation and release of a metalloproteinase. We observed that binding of EphB2 to ephrin-B1 promotes secretion of MMP-8 without increasing the expression level of MMP-8. Activation of several molecules, such as Erk, p38 and PI 3-kinase or Akt cause transcriptional activation of metalloproteinases (Chinni et al., 2006; Raymond et al., 2006; Reuben and Cheung, 2006). In our study, however, activation of ephrin-B1 by EphB2 binding did not alter the phosphorylation levels of Erk-1, 2, p38 or Akt (data not shown), as also reported by others (Huynh-Do et al., 2002). Our observation that ephrin-B1-induced secretion of MMP-8 was sensitive to brefeldin A, which blocks the membrane trafficking of coated vesicles at the Glogi/trans-Golgi network suggests that ephrin-B1 signaling resulted in increased transport of MMP-8 from the cytoplasm to the cell surface (Tamaki and Yamashina, 2002).

Regulation of the secretion of MMP-8 enables ephrin-B1 signaling to play an important role in regulating MMP-8 activity. Like other soluble MMPs, MMP-8 is proteolytically activated extracellularly by removal of its propeptide domain, and physiologically relevant level of MMP protease activity requires efficient release of the protease to the cellular surface (Sternlicht and Werb, 2001). Although the molecular mechanism of the MMP-8 secretory pathway is not well understood, our data indicate that signaling mediated by the carboxyl-terminal region of ephrin-B1 is involved. Notably, removal of the C-terminus of ephrin-B1 resulted in significant reduction of MMP-8 secretion and cleavage of the extracellular domain of ephrin-B1. In addition, the C-terminus of ephrin-B1 regulates the signal leading to activation of Arf1, a critical regulator of membrane traffic in the secretory pathway and one target of brefeldin A (Tamaki and Yamashina, 2002; Donaldson

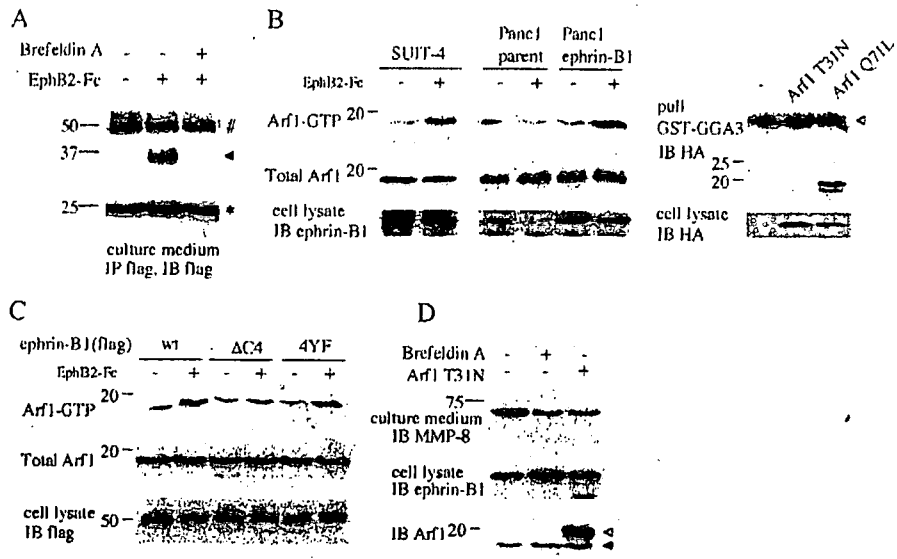

Fig. 6. Stimulation of ephrin-B1 with EphB2 activates Arf1. (A) Flag-tagged ephrin-B1 was expressed in Capan-1 cells. The cells were treated with or without EphB2-Fc (2 μg/ml) and brefeldin A (10 μg/ml) as indicated for 1.5 hours, and conditioned medium was assayed for the 35 kDa ectodomain of ephrin-B1. (B,C) The activity of Arf1 was analyzed in the indicated cells. (C) Wild-type or mutant ephrin-B1 was expressed in Capan-1 cells as in Fig. 2A. The cells were incubated with EphB2-Fc (4 μg/ml) for 20 minutes before being lysed. Arf1-GTP was pulled down with GST-GGA3 bound to glutathione-Sepharose. As controls, lysates of COS-1 cells transiently transfected with plasmids encoding Arf1 T31N or Arf1 Q71L, HA tagged at the C-terminus were analyzed (B, right panel). Open arrowhead indicates cross-reacted GST-GGA3 used for the pull-down assay. (D) Suppression of Arf1 activation decreased the MMP-8 secretion. Capan-1 cells stably expressing ephrin-B1 were used. In the right lane, Arf1 T31N was also transiently expressed in the cells by retrovirus mediated gene transfer. All cells were treated with EphB2-Fc together with (middle lane) or without brefeldin A for 4 hours, and the conditioned medium was subjected to TCA precipitation to detect MMP-8 through immunoblotting. The filled arrowhead indicates endogenous Arf1, and the open arrowhead indicates HA-tagged Arf1 T31N (bottom).

et al., 2005). Arf1 GTPase regulates the membrane association of coat proteins involved in intracellular membrane trafficking, which is critical for the vesicle transport of secretory proteins at the Golgi (Donaldson et al., 2005). Actually we observed that treatment of cells with brefeldin A, or expression of Arf1 T31N inhibited the secretion of MMP-8. Therefore, as one possibility, secretion of MMP-8 is upregulated by activation of Arf1 GTPase through ephrin-B1 signaling, although the molecular mechanisms connecting ephrin-B1 and Arf1 are still not well understood. As ephrin-B1 has a docking site for the PDZ domain at the C-terminus, some protein containing PDZ domains may be involved in this pathway. As a consequence, the increase of secreted MMP-8 may trigger the degradation of extracellular matrix and the cleavage of ephrin-B1 as a possible feedback mechanism (Fig. 8). In our preliminary observations, Arf1 activation occurs as fast as 10 minutes after stimulation with EphB2-Fc, and some increase of MMP-8 in the culture medium was detected from 0.5 hours after addition of EphB2-Fc. By contrast, the cleavage of ephrin-B1 was observed at 1 hour, but not at 10 minutes after stimulation with EphB2-Fc, by immunoblotting of a cleaved C-terminal fragment of ephrin-B1, p17, in cell lysates (data not shown). Although we cannot determine the precise time point of MMP-8 secretion because of the limitation of the antibody's sensitivity, these observations are compatible with the model that ephrin-B1 reverse signaling induces Arf1 activation, which leads to MMP-8 release and ephrin-B1 cleavage. As extracellular activation of MMPs can be triggered by activation of other MMPs, there is the possibility that ephrin-B1-mediated signaling may synergistically promote activity of several MMPs. In addition, Arf1 GTPase may involve the intracellular transport of not only MMP-8, but also several other MMPs. Whether metalloproteinases other than MMP-8 are also upregulated by EphB2 stimulation of ephrin-B1 should also be investigated.

We show that the 35 kDa ephrin-B1 fragment in the culture medium of SUIT-4 cells was generated by cleavage at aa 218. From the experiments using natural inhibitors of metalloproteinases, TIMP-1 but not TIMP-2 and TIMP-3 effectively blocked the cleavage of ephrin-B1. Among these TIMPs, TIMP-3 most effectively inhibits the function of ADAM family metalloproteinase, including ADAM-17 (TACE), ADAM-10 and ADAM-TS4 (Amour et al., 2000; Brew et al., 2000; Hashimoto et al., 2001). In addition, membrane-type metalloproteinases (MT-MMPs) are preferentially inhibited by TIMP-2 and TIMP-3, but not by TIMP-1 (Brew et al., 2000). Our observation that cleavage of ephrin-B1 was most effectively inhibited by TIMP-1, but not by TIMP-2 or TIMP-3 suggests that it is unlikely that those members of the ADAMs family are critically involved. However, we cannot exclude that TIMP-3-independent ADAM metalloproteinases may contribute to the processing of ephrin-B1. Together with the observation that ephrin-B1 cleavage was at least partially inhibited by RNA interference of MMP-8, and it was increased by overexpression of MMP-8, our results suggest that MMP-8 is the key metalloproteinase that cleaves ephrin-B1 ectodomain.

In addition to an extracellular 35 kDa peptide derived from the N-terminal of ephrin-B1, stimulation of ephrin-B1-expressing cells with EphB2-Fc resulted in the production of a 17 kDa intracellular fragment (p17) derived from the C-terminus of ephrin-B1. As detection of p17 was abolished in L cells expressing the ephrin-B1 4A mutant (data not shown), p17 was generated by cleavage of ephrin-B1 within the extracellular domain at aa 218. Ephrin-B1 and ephrin-B2 are cleaved within the transmembrane region by presenilin-dependent γ-secretase, which releases an approximately 12

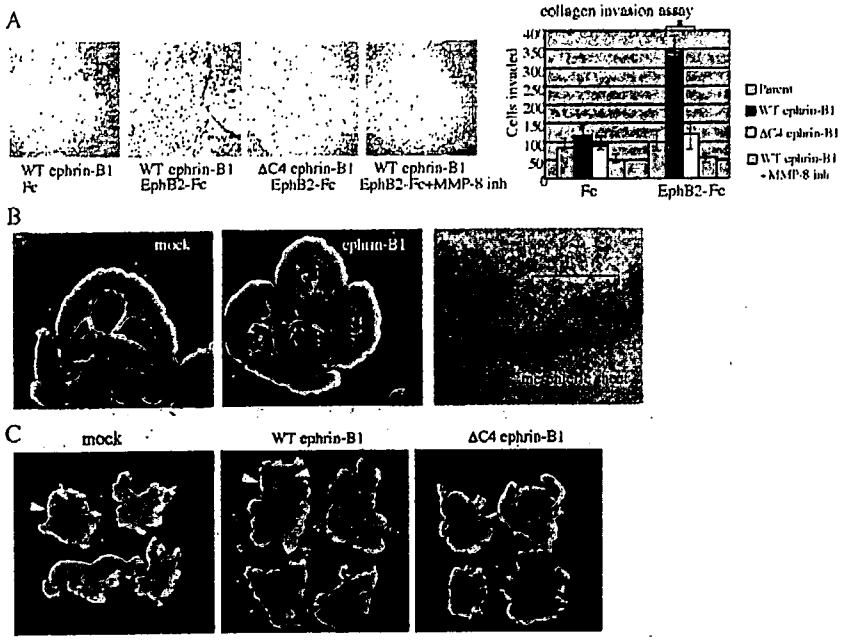

Fig. 7. The C-terminus of ephrin-B1 regulates the invasion of cancer cells. (A) Wild-type (WT) ephrin-B1 or ΔC4 ephrin-B1 mutant was expressed in Capan-1 cells. The cells were seeded onto a Transwell membrane coated with a collagen matrix (25 μg/ cm^2) in serum-free medium containing control Fc or EphB2-Fc (4 μg/ml) with or without addition of the MMP-8 inhibitor (1 μM). In the lower chamber, medium containing 5% FBS was added as a chemoattractant. After 8 hours incubation, the wells were harvested and cells that had invaded the collagen were counted. Representative fields are shown. (Right) The results from three independent experiments, each in duplicate, are shown as the mean ± s.d. *P<0.01. (B) PANC-1 ephrin-B1 cells or PANC-1 cells transfected with a mock vector (mock) were injected intraperitoneally into nude mice. The representative appearance of intestinal loops 8 weeks after injection is shown. Arrows indicate disseminated tumor nodules in the mesentery. The right panel shows the histology of the tumors in the mesentery (×100). The asterisk indicates a tumor nodule. Microscopic invasion of cancer cells was observed in the mesenteric sheet (blanket). (C) Representative appearance of the tumors of panc1 cells expressing either mock vector, wild-type or ΔC4 ephrin-B1 in the rectouterine region was compared. Yellow and red arrowheads indicate uterine horns and tumor nodules, respectively.

kDa intracellular fragment (Georgakopoulos et al., 2006; Tomita et al., 2006). Although p17 may be further processed by γ-secretase and produce a small intracellular peptide, we did not detect such a product, possibly because of its rapid degradation or cell type-dependent differences in protease activity.

One possible function of ephrin-B1-mediated MMP-8 secretion is processing of ephrin-B1 and downregulation of EhpB2-stimulated ephrin-B1 intracellular signaling. Unlike wild-type ephrin-B1 protein, ΔC ephrin-B1 protein was not reduced after EphB2-Fc treatment, which seems to suggest that cleavage of ephrin-B1 contributes to the down regulation of ephrin-B1 after stimulation. However, recent reports show the trans-endocytosis of ephrin-B1 after engagement with EphB receptors, which regulates ephrin-B-mediated cell repulsion (Zimmer et al., 2003; Marston et al., 2003; Parker et al., 2004). We also observed that ephrin-B1 4A, which also triggers Arf1 activation and release of MMP-8, but is resistant to cleavage, was degraded and decreased in amount after stimulation with EphB2-Fc almost to the same degree with wild-type ephrin-B1 (data not shown). Because the C-terminus of ephrin-B1 may also modify its endocytosis, we cannot conclude at present that ephrin-B1 cleavage greatly affects the stability and turnover of the EphB-ephrin-B1 complex on the cell surface. Rather, the biological significance of ephrin-B1-mediated MMP-8 secretion is considered to be the promotion of the invasion potential of cancer cells via degradation of surrounding extracellular matrix. However, addition of the 35 kDa ephrin-B1 ectodomain prepared from conditioned medium of ephrin-B1 expressing COS-1 cells inhibited the motility of EphB2-expressing cells, similar to the effect of unclustered ephrin-B1-Fc, indicating the possible biological effect of secreted fragments on cell movement, whereas it did not affect cell proliferation (see Fig. S2 in supplementary material).

Table 1. Mesenterial dissemination after intraperitoneal inoculation of cancer cells

	Number of nodules*		
Cell line	0-10	10-30	30+
Mock	16	2	0
WT ephrin-B1	0	4	17
ΔC4 ephrin-B1	12	4	3

Data are shown as the number of mice with tumors in the mesentery.
*Number of tumor nodules larger than 2 mm in the mesentery per body.

The potential significance of ephrin-B1 in cancer cell invasion is supported by our finding that ephrin-B1-mediated collagen invasion by Capan-1 cells was related to MMP-8. The inability of ΔC-ephrin-B1 to promote collagen invasion in the same assay revealed that signaling through C-terminus of ephrin-B1 affects the invasion ability of cancer cells. In addition, expression of ephrin-B1 in the pancreas cancer cells, PANC-1, promoted the dissemination of intraperitoneally injected cells into the mesentery and peritoneal cavity where they formed tumor nodules, demonstrating for the first time that ephrin-B1 actually promotes cancer cell invasion in vivo. Overexpression of B-type ephrins in cancer cells would affect cell-cell adhesion by their interaction with cell adhesion proteins such as claudin (Tanaka et al., 2005). Ephrin-B1-mediated intracellular signaling also results in aberrant

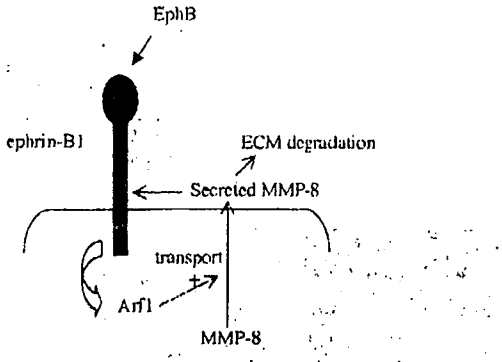

Fig. 8. Diagram showing the possible mechanism of ephrin-B1-mediated stimulation of MMP-8 secretion and cell invasion. When ephrin-B1 is stimulated by EphB receptors, Arf1 GTPase is activated through signaling mediated by the C-terminus ephrin-B1, which may stimulate the transport of MMP-8 for extracellular release. The increase of secreted MMP-8 triggers the degradation of extracellular matrix (ECM) and cleavage of ephrin-B1.

activation of RhoA and Rac1 (Tanaka et al., 2003; Tanaka et al., 2004; Lee et al., 2005). Together, events such as these would result in increased cell motility. These findings in conjunction with the ephrin-B1 induction of MMP-8 secretion, indicate that ephrin-B1 overexpression would result in an enhanced potential for invasion of surrounding tissues. For example, both MMP-8 and ephrin-B1 are frequently expressed in ovarian cancers, and their expression correlates with tumor grade and a poor prognosis (Castellvi et al., 2006; Varelias et al., 2002). Ephrin-B1 could also be involved in invasion of cancer cells circulating in the blood into sheets of endothelial cells which express EphB receptors and play a role in extravasation and metastasis. The inhibition of a specific cellular signal originating in ephrin-B1 stimulation may be a good candidate for regulating tumor invasion.

Materials and Methods

Plasmids, antibodies and reagents

Plasmids encoding full-length cDNAs of human ephrin-B1 and the Fc fusion protein construct of EphB2 and ephrin-B1 have been described previously (Tanaka et al., 2004). Fc fusion proteins were purified from the culture medium of COS-1 cells transfected with plasmids encoding EphB2-Fc or ephrin-B1-Fc using a protein A Sepharose column as described previously (Tanaka et al., 2004). Mutants of ephrin-B1 lacking the cytoplasmic tail (ΔC4 and ΔC19, truncation of four or 19 aa residues at the C-terminus, respectively) were generated using PCR-based techniques. Alanine substitution of four aa in the extracellular domain (aa 216-219) of ephrin-B1, ephrin-B1 4A, was performed using the Altered Sites Mutagenesis System (Promega). Generation of Ephrin-B1 with mutations of four tyrosine residues in the cytoplasmic domain (Y313, 317, 324, 329) and ephrin-B1 4YF, have been described previously (Tanaka et al., 2005). For making flag-tagged ephrin-B1, a DNA fragment encoding the Flag tag was inserted 3′ to the signal peptide of ephrin-B1 (aa 1-24). To generate a plasmid encoding human activated MMP-8, cDNA corresponding to nucleotides 336-824 of the reported sequence (GenBank accession number BC074988) was amplified with RT-PCR from a cDNA template derived from U937 cells. The amplified MMP-8 cDNA was tagged with the signal peptide and Flag at the 5′ terminus, and cloned into pcDNA3. GST-GGA3 was generated by cloning of PCR-amplified cDNA corresponding to aa 1-313 of human GGA3 short isoform (GenBank accession number AF219139) into pGEX4T2 (Amersham Pharmacia). The plasmids encoding wild-type Arf1 and Arf1 T31N bearing the HA epitope at the C-terminus were donated from J. S. Bonifacino (National Institute of Child Health and Human Development, NIH, Bethesda, MA). To generate the recombinant retrovirus, cDNAs were subcloned into pDON-AI vector (Takara). Monoclonal and polyclonal antibodies that recognize the Flag tag were purchased from Sigma and Affinity Bioreagents (Affinity Bioreagents, Golden, CO), respectively. Antibodies that recognize the HA tag were from InvivoGen (InvivoGen, San Diego, CA; monoclonal antibody) and Santa Cruz Biotechnology Inc. (polyclonal antibody). Rabbit polyclonal antibody that recognizes ephrin-B1 (C18) was purchased from Santa Cruz Biotechnology, Inc. The goat polyclonal antibody against ephrin-B1, which reacts with the entire extracellular domain, was purchased from R&D Systems. The polyclonal antibody against tyrosine-phosphorylated ephrin-B1 (ephrin-B1 pY317, aa residues 314-321) was raised in rabbits and affinity-purified as described previously (Tanaka et al., 2005). EphB2 and EphB4 polyclonal antibodies were from R&D Systems. Polyclonal and mouse monoclonal antibodies for MMP-8 were purchased from Chemicon and Daiichi Fine Chemical (Takaoka, Japan), respectively. The monoclonal antibody for phosphotyrosine (4G10) and Arf1 was from Upstate Biotechnology and Affinity Bioreagents, respectively. TrueBlot anti-rabbit IgG secondary antibody was purchased from eBioscience (San Diego, CA). Cyclohexamide and actinomycin D were purchased from Sigma. Purified TIMP-1, and 2 were purchased from Calbiochem, and TIMP-3 was from Sigma. The protease inhibitors shown in Fig. 3 and purified MMP-1 (proenzyme), MMP-8 (proenzyme), MT1-MMP (catalytic domain, aa 89-265) and ADAM10 (mature active ectodomain, aa 19-673) were purchased from Calbiochem. The MMP-8 inhibitor is (3R)-(+)-[2-(4-methoxybenzenesulfonyl)-1,2,3,4-tetrahydroisoquinoline-3-hydroxamate]. Src family kinase inhibitor 4-amino-5-(4-chlorophenyl)-7-(t-butyl)pyrazolo[3,4-d]pyrimidine (PP2) and the structural analog 4-amino-7-phenylpyrazolo[3,4-d]pyrimidine (PP3) were purchased from Calbiochem.

Cell culture, transfection and retrovirus infection

SUIT-4 (Kawano et al., 2004) and the other pancreas carcinoma cell lines were cultured in RPMI1640 supplemented with 10% fetal bovine serum. Mice fibroblast L cells and COS-1 cells were cultured in DMEM with 10% fetal bovine serum. For transient expression assays, COS-1 cells and SUIT-4 cells were transfected with plasmid DNA using Lipofectamine 2000 reagent (Invitrogen). Recombinant retroviral plasmid, pDON-AI was cotransfected with pCL-10A1 retrovirus packaging vector (IMGENEX) into 293gp cells to allow the production of retroviral particles. Capan-1 cells were infected with retroviruses for transient expression of ephrin-B1 or Arf1 mutants, and used for experiments 48 hours after infection. For some experiments, Capan-1 cells stably expressing wild-type ephrin-B1 were established after retrovirus infection through the selection in medium containing G418 (600 μg/ml). L cells stably expressing ephrin-B1 or EphB2 were established as described and cultured in medium containing hygromycin B at a concentration of 400 μg/ml (Tanaka et al., 2005). PANC-1 cells stably expressing ephrin-B1 were established through selection in medium containing puromycin at a concentration of 2 μg/ml for 2-3 weeks. Well isolated colonies were characterized further.

In vitro siRNA treatment

Stealth siRNA (Invitrogen) of MMP-8 was synthesized as follows. Sense: 5′-AAGGCAUGAGCAAGGAUUCCAUUGG-3′; antisense: 5′-CCAAUGGAAUCC-UUGCUCAUGCCUU-3′. The control siRNA (scramble II duplex: 5′-GCG-CGCUUUGUAGGAUUCGdTdT-3′) was purchased from Dharmacon. SiRNAs were incorporated into cells using Lipofectamine™ 2000 according to the manufacturer's instructions (Invitrogen). Assays were performed 72 hours post treatment.

Peptidomic analysis of secretory proteins

SUIT-4 cells were cultured in serum-free RPMI1640 medium and the conditioned medium was collected. Cleared supernatant was loaded onto a SepPak C18 cartridge (Waters) for peptide extraction. Peptides bound to the cartridge were eluted with 0.1% trifluoroacetic acid (TFA)/60% acetonitrile (ACN) and lyophilized. The resultant sample was reconstituted with the same solvent and applied to an HPLC gel filtration column (Pharmacia). Fractions containing peptides with a molecular mass below 8,000 Da were subjected to reductive alkylation as described previously (Sasaki et al., 2002) and desalted with an Empore disk cartridge (3M). The desalted material was separated with a 75 mm × 100 mm C18 column (LC Packings, Sunnyvale, CA) before matrix assisted laser desorption ionisation (MALDI)-MS/MS analysis using an Ultimate HPLC pump and gradient programmer (LC Packings). The solvent system was 5% acetonitrile (ACN) (solvent A) and 95% ACN (solvent B); both contained 0.1% TFA. A linear gradient from 5% B to 60% B over 50 minutes was used. Eluates were spotted at 20-second intervals using Probot (LC Packings) on a MALDI target plate. Mass spectra were obtained in reflector mode on a (MALDI-TOF/TOF 4700 mass spectrometer (Applied Biosystems). Ion signals above S/N 25 observed in the MSMS spectra were selected for MSMS ion search against human entries in the NCBI nr database using the Mascot (Matrix Science) search algorithm with no enzyme specification, with the mass tolerance of precursor ions and product ions set at 100 ppm and 0.25 Da, respectively.

Immunoprecipitation and immunoblotting

Cell lysates were prepared with protease inhibitors in PLC buffer [50 mM HEPES (pH 7.5), 150 mM NaCl, 1.5 mM $MgCl_2$, 1 mM EGTA, 10% glycerol, 100 mM NaF, 1 mM Na_3VO_4 and 1% Triton X-100]. To precipitate the proteins, 1 μg of

monoclonal or affinity purified polyclonal antibody was incubated with 500 μg of cell lysate for 2 hours at 4°C, and then precipitated with protein G agarose for 1 hr at 4°C. Immunoprecipitates were extensively washed with PLC buffer, separated by SDS-PAGE, and immunoblotted. In some experiments, TrueBlot anti-rabbit IgG (eBioscience), which does not react to the denatured rabbit IgG, was used as the secondary antibody of the immunoblotting. For detection of MMP-8, rabbit polyclonal antibody was basically used in this study, however, almost the same results were obtained by using mouse monoclonal antibody.

RT-PCR

Total RNA was prepared from cultured cells by Isogen (Nippon Gene) according to the manufacturer's instructions and treated with DNase I. cDNA was synthesized from 2 μg of total RNA, and polymerase chain reactions (PCR) were performed in a 25 μl reaction volume at an annealing temperature of 55°C. The linear area of the PCR for each reaction was defined; 15 cycles for GAPDH and 25 cycles for MMP-8. Specific primers for MMP-8 and GAPDH have been described previously (Wahlgren et al., 2001; Woo et al., 2003); the expected PCR products were 352 bp and 300 bp, respectively. PCR products were subjected to electrophoresis on 2% agarose gels, and DNA was visualized by ethidium bromide staining.

Metabolic labeling

Cells cultured in 60 mm diameter dishes were preincubated in methionine-free DMEM (Sigma) for 1 hour, then cultured in 1.5 ml of methionine-free medium containing 0.15 mCi of [^{35}S]methionine (Amersham) for a further 4 hours. The cells were rinsed extensively and incubated in medium supplemented with EphB2-Fc or control Fc at 4 μg/ml for 2 hours. MMP-8 in the conditioned medium was purified by immunoprecipitation using an anti-MMP-8 polyclonal antibody and separated on SDS-PAGE. The gel was dried and subjected to autoradiography. The results were visualized with a Bio Imaging Analyzer (BAS1000; Fuji).

In vitro cleavage of ephrin-B1

Purified MMP-1 and MMP-8 were activated prior to use by treatment with 2 mM *p*-aminophenylmercuric acetate for 90 minutes at 37°C and dialyzed against 50 mM Tris-HCl (pH 7.5) containing 150 mM NaCl, 5 mM $CaCl_2$ and 50 μM $ZnCl_2$. Activated enzymes (10 nM, each) were incubated with ephrin-B1-Fc (2 μM) in 50 mM Tris-HCl (pH 7.5) containing 150 mM NaCl, 5 mM $CaCl_2$, 50 μM $ZnCl_2$ and 0.05% SDS at 37°C for 1 hour, separated by SDS-PAGE, and immunoblotted with anti-Fc of mouse IgG.

Arf1-GTP pull-down assay

To assess the amount of activated Arf1-GTP in cells, we performed a pull-down assay by using a GST-GGA3 construct (Dell's Angelica et al., 2000). Briefly, cells were left untreated or treated with EphB2-Fc (4 μg/ml) for 20 minutes. Cell lysates were prepared in lysis buffer [50 mM HEPES (pH 7.5), 150 mM NaCl, 10 mM $MgCl_2$, 10% glycerol, 100 mM NaF, 1 mM Na_3VO_4 and 1% Triton X-100], and then incubated with gluthathione-Sepharose beads containing a GST-GGA3 fusion protein for 45 minutes at 4°C. Precipitates were washed four times in the same buffer, and the precipitated Arf1 was detected by immunoblotting.

In vivo tumor invasion assay

The animal experimental protocols were approved by the Committee for Ethics of Animal Experimentation, and the experiments were conducted in accordance with the guidelines for Animal Experiments of the National Cancer Center. Peritoneal dissemination of tumors was tested by intraperitoneal injection of 1×10^7 PANC-1 cells suspended in 0.3 ml of RPMI1640 medium into 6-week-old BALB/c nude mice (CLEA Japan, Inc.). The mice were sacrificed 8 weeks after injection, and peritoneal dissemination was evaluated. To examine expression of Eph receptors in mesentery-derived cells, the mesenteric sheets were cut along the streak of arteries as described previously (Akedo et al., 1986). The cells were collected from dissected sheets by incubating at 37°C for about 20 minutes in 0.25% trypsin in PBS.

We thank D. B. Alexander (Department of Molecular Toxicology, Nagoya City University) for useful discussions and critical reading of this manuscript. We thank J. S. Bonifacino (National Institute of Child Health and Human Development, NIH) for donating Arf1 plasmids. This work was supported by the Program for the Promotion of Fundamental Studies in Health Science of the Organization for Pharmaceutical Safety and Research of Japan.

References

Akedo, H., Shinkai, K., Mukai, M., Mori, Y., Tateishi, R., Tanaka, K., Yamamoto, R. and Morishita, T. (1986). Interaction of rat ascites hepatoma cells with cultured mesothelial cell layers: a model for tumor invasion. *Cancer Res.* **46**, 2416-2422.

Amour, A., Knight, C. G., Webster, A., Slocombe, M., Stephens, P. E., Knauper, V., Docherty A. J. P. and Murphy, G. (2000). The in vitro activity of ADAM-10 is inhibited by TIMP-1 and TIMP-3. *FEBS Lett.* **473**, 275-279.

Batlle, E., Henderson, J. T., Beghtel, H., Van den Born, M., Sancho, E., Huls, G., Meeldijk, J., Robertson, J., Van de Wetering, M., Pawson, T. et al. (2002). Beta-catenin and TCF mediate cell positioning in the intestinal epithelium by controlling the expression of EphB/ephrinB. *Cell* **111**, 251-263.

Batlle, E., Bacani, J., Begthel, H., Jonkheer, S., Gregorieff, A., Van den Born, M., Malats, N., Sancho, E., Boon, E., Pawson, T. et al. (2005). EphB receptor activity suppresses colorectal cancer progression. *Nature* **435**, 1126-1130.

Blits-Huizinga, C., Nelersa, C., Malhotra, A. and Liebl, D. (2004). Ephrins and their receptors: binding versus biology. *IUBMB Life* **56**, 257-265.

Bong, Y. S., Park, Y. H., Lee, H. S., Mood, K., Ishimura, A. and Daar, I. O. (2004). Tyr-298 in ephrin-B1 is critical for an interaction with the Grb4 adaptor protein. *Biochem. J.* **377**, 499-507.

Brew, K., Dinakarpandian, D. and Nagase, H. (2000). Tissue inhibitors of metalloproteinases: evolution, structure and function. *Biochem. Biophys. Acta* **1477**, 267-283.

Castellvi, J., Garcia, A., De la Torre, J., Hernandez, J., Gil, A., Xercavins, J. and Cajal, S. R. (2006). EphrinB expression in epithelial ovarian neoplasms correlates with tumor differentiation and angiogenesis. *Hum. Pathol.* **37**, 883-889.

Chinni, S. R., Sivalogan, S., Dong, Z., Trindade Filho, J. C., Deng, X., Bonfil, R. D. and Cher, M. L. (2006). CXCL12/CXCR4 signaling activates Akt-1 and MMP-9 expression in prostate cancer cells: the role of Bone microenvironment-associated CXCL12. *Prostate* **66**, 32-48.

Cowan, C. A. and Henkemeyer, M. (2001). The SH2/SH3 adaptor Grb4 transduces B-ephrin reverse signals. *Nature* **413**, 174-179.

Dell'Angelica, E. C., Puertollano, R., Mullins, C., Aguilar, R. C., Vargas, J.D., Hartnell, L. M. and Bonifacino, J.S. (2000). GGAs: a family of ADP ribosylation factor-binding proteins related to adaptors and associated with the Golgi complex. *J. Cell Biol.* **149**, 81-93.

Donaldson, J. G. (2005). Arfs, phosphoinositides and membrane traffic. *Biochem. Soc. Trans.* **33**, 1276-1278.

Georgakopoulos, A., Litterst, C., Ghersi, E., Baki, L., Xu, C. J., Serban, G. and Robakis, N. K. (2006). Metalloproteinase/Presenilin1 processing of ephrinB regulates EphB-induced Src phosphorylation and signaling. *EMBO J.* **25**, 1242-1252.

Hashimoto, G., Aoki, T., Nakamura, H., Tanzawa, K. and Okada, Y. (2001). Inhibition of ADAMTS4 (aggrecanase-1) by tissue inhibitors of metalloproteinases (TIMP-1, 2, 3 and 4). *FEBS Lett.* **494**, 192-195.

Hattori, M., Osterfield, M. and Flanagan, J. G. (2000). Regulated cleavage of a contact-mediated axon repellent. *Science* **289**, 1360-1365.

Holmberg, J., Genander, M., Halford, M. M., Anneren, C., Sondell, M., Chumley, M. J., Silvany, R. E., Henkemeyer, M. and Frisen, J. (2006). EphB receptors coordinate migration and proliferation in the intestinal stem cell niche. *Cell* **125**, 1151-1263.

Huynh-Do, U., Vindis, C., Liu, H., Cerretti, D. P., McGrew, J. T., Enriquez, M., Chen, J. and Daniel, T. O. (2002). Ephrin-B1 transduces signals to active integrin-mediated migration, attachment and angiogenesis. *J. Cell Sci.* **115**, 3073-3081.

Janes, P. W., Saha, N., Barton, W. A., Kolev, M. V., Wimmer-Kleikamp, S. H., Nievergall, E., Blobel, C. P., Himanen, J. P., Lackmann, M. and Nikolov, D. B. (2005). Adam meets Eph: an ADAM substrate recognition module acts as a molecular switch for ephrin cleavage in trans. *Cell* **123**, 291-304.

Kataoka, H., Tanaka, M., Kanamori, M., Yoshii, S., Ihara, M., Wang, Y. J., Song, J. P., Li, Z. Y., Arai, H., Otuki, Y.et al. (2002). Expression profile of EFNB1, EFNB2, two ligands of EPHB2 in human gastric cancer. *J. Cancer Res. Clin. Oncol.* **128**, 343-348.

Kawano, K., Iwamura, T., Yamarari, H., Seo, Y., Suganuma, T. and Chijiiwa, K. (2004). Establishment and characterization of a novel human pancreatic cancer cell line (SUIT-4) metastasizing to lymph nodes and lungs in nude mice. *Oncology* **66**, 458-467.

Klein, R. (2004). Eph/ephrin signaling in morphogenesis, neural development and plasticity. *Curr. Opin. Cell Biol.* **16**, 580-589.

Lee, H. S., Bong, Y. S., Moore, K. B., Soria, K., Moody, S. A. and Daar, I. O. (2005). Dishevelled mediates ephrinB1 signalling in the eye field through the planar cell polarity pathway. *Nat. Cell Biol.* **8**, 55-63.

Lin, D., Gish, G. D., Songyang, Z. and Powson, T. (1999). The carboxyl terminus of B class ephrins constitutes a PDZ domain binding motif. *J. Biol. Chem.* **274**, 3726-3733.

Lint, P. V. and Libert, C. (2006). Matrix metalloproteinase-8: cleavage can be decisive. *Cytokine Growth Factor Rev.* **17**, 217-223.

Marston, D. J., Dickinson, S. and Nobes, C. D. (2003). Rac-dependent trans-endocytosis of ephrinBs regulates Eph-ephrin contact repulsion. *Nat. Cell Biol.* **5**, 879-888.

Meyer, S., Hafner, C., Guba, M., Flegel, S., Geissler, E. K., Becker, B., Koehl, G., Orso, E., Landthaler, M. and Vogt, T. (2005). Ephrin-B2 overexpression enhances integrin-mediated ECM-attachment and migration of B16 melanoma cells. *Int. J. Oncol.* **27**, 1197-1206.

Murai, K. K. and Pasquale, E. B. (2003). Ephective signaling: forward, reverse and crosstalk. *J. Cell Sci.* **116**, 2823-2832.

Nakada, M., Drake, K. L., Nakada, S., Niska, J. A. and Berens, M. E. (2006). Ephrin-B3 ligand promotes glioma invasion through activation of Rac1. *Cancer Res.* **66**, 8492-8500.

Niu, T. K., Pfeifer, A. C., Lippincott-Schwartz, J. and Jackson, C. L. (2005). Dynamics of GBF1, a Brefeldin A-sensitive Arf1 exchange factor at the Golgi. *Mol. Biol. Cell* **16**, 1213-1222.

Parker, M., Roberts, R., Enriquez, M., Zhao, X., Takahashi, T., Pat, C., Daniel, T. and Chen, J. (2004). Reverse endocytosis of transmembrane ephrin-B ligands via a clathrin-mediated pathway. *Biochem. Biophys. Res. Commun.* **323**, 17-23.

Pascall, J. C. and Brown, K. D. (2004). Intramembrane cleavage of ephrinB3 by the

human rhomboid family protease, RHBDL2. *Biochem. Biophys. Res. Commun.* 317, 244-252.

Poliakov, A., Cotrina, M. and Wilkinson, D. G. (2004). Diverse roles of Eph receptors and ephrins in the regulation of cell migration and tissue assembly. *Dev. Cell* 7, 465-480.

Raymond, L., Eck, S., Mollmark, J., Hays, E., Tomek, L., Kantor, S., Elliott, S. and Vincenti, M. (2006). Interleukin-1 beta induction of matrix metalloproteinase-1 transcription in chondrocytes requires ERK-dependent activation of CCAAT enhancer-binding protein-beta. *J. Cell. Physiol.* 207, 683-688.

Reuben, P. M. and Cheung, H. S. (2006). Regulation of matrix metalloproteinase (MMP) gene expression by protein kinases. *Front. Biosci.* 11, 1199-1215.

Sasaki, K., Sato, K., Akiyama, Y., Yanagihara, K., Oka, M. and Yamaguchi, K. (2002). Peptidomics-based approach reveals the secretion of the 29-residue COOH-terminal fragment of the putative tumor suppressor protein DMBT1 from pancreatic adenocarcinoma cell lines. *Cancer Res.* 62, 4894-4898.

Sawicki, G., Leon, H., Sawicka, J., Sariahmetoglu, M., Schulze, C. J., Scott, P. G., Szczesna-Cordary, D. and Schulz, R. (2005). Degradation of myosin light chain in isolated rat hearts subjected to ischemia-reperfusion injury. *Circulation* 112, 544-552.

Siller-Lopez, F., Garcia-Banuelos, J., Hasty, K. A., Segura, J., Ramos-Marquez, M., Qoronfleh, M. W., Aguilar-Cordova, E. and Armendariz-Borunda, J. (2000). Truncated active matrix metalloproteinase-8 gene expression in HepG2 cells is active against native type I collagen. *J. Hepatol.* 33, 758-763.

Stadlemann, S., Pollheimer, J., Moser, P. L., Raggi, A., Amberger, A., Margreiter, R., Offner, F. A., Mikuz, G., Dirnhofer, S. and Moch, H. (2003). Cytokine-regulated expression of collagenase-2 (MMP-8) is involved in the progression of ovarian cancer. *Eur. J. Cancer* 39, 2499-2505.

Sternlicht, M. D. and Werb, Z. (2001). How matrix metalloproteinases regulate cell behavior. *Annu. Rev. Cell Dev. Biol.* 17, 463-516.

Tamaki, H. and Yamashina, S. (2002). The stack of the Golgi apparatus. *Arch. Histol. Cytol.* 65, 209-218.

Tanaka, M., Kamo, T., Ota, S. and Sugimura, H. (2003). Association of dishevelled with Eph tyrosine kinase receptor and ephrin mediates cell repulsion. *EMBO J.* 22, 847-858.

Tanaka, M., Ohashi, R., Nakamura, R., Shinmura, K., Kamo, T., Sakai, R. and Sugimura, H. (2004). Tiam1 mediates neurite outgrowth induced by ephrin-B1 and EphA2. *EMBO J.* 23, 1075-1088.

Tanaka, M., Kamata, R. and Sakai, R. (2005). Phosphorylation of ephrin-B1 via the interaction with claudin following cell-cell contact formation. *EMBO J.* 24, 3700-3711.

Tomita, T., Tanaka, S., Morohashi, Y. and Iwatsubo, T. (2006). Presenilin-dependent intramembrane cleavage of ephrin-B1. *Mol. Neurodegener.* 1, 2.

Varelias, A., Koblar, S. A., Cowled, P. A., Carter, C. D. and Clayer, M. (2002). Human osteosarcoma express specific ephrin profiles: implications for tumorigenicity and prognosis. *Cancer* 95, 862-869.

Wahlgren, J., Maisi, P., Sorsa, T., Sutinen, M., Tervahartiala, T., Pirila, E., Teronen, O., Hietanen, J., Tjaderhane, L. and Salo, T. (2001). Expression and induction of collagenases (MMP-8 and -13) in plasma cells and associated with bone-destructive lesions. *J. Pathol.* 194, 217-224.

Woo, J. H., Park, J. W., Lee, S. H., Kim, Y. H., Lee, I. K., Gabrielson, E., Lee, S. H., Lee, H. J., Kho, Y. H. and Won, T. K. (2003). Dykellic acid inhibits phorbol myristate acetate-induced matrix metalloproteinase-9 expression by inhibiting nuclear factor kappa B transcriptional activity. *Cancer Res.* 63, 3430-3434.

Yu, W. H., Woessner, J. F., McNeish, J. D. and Stamenkovic, I. (2007). CD44 anchors the assembly of matrilysin/MMP-7 with heparin-binding epidermal growth factor precursor and ErbB4 and regulates female reproductive organ remodeling. *Genes Dev.* 16, 307-323.

Zeeh, J. C., Zeghouf, M., Grauffel, C., Guilbert, B., Martin, E., Dejaegere, A. and Cherfils, J. (2006). Dual specificity of the interfacial inhibitor Brefeldin A for Arf proteins and Sec7 domains. *J. Biol. Chem.* 281, 11805-11814.

Zimmer, M., Palmer, A., Kohler, J. and Klein, R. (2003). EphB-ephrinB bi-directional endocytosis terminates adhesion allowing contact mediated repulsion. *Nat. Cell Biol.* 5, 869-878.

MOLECULAR AND CELLULAR BIOLOGY, Nov. 2007, p. 7649–7660 Vol. 27, No. 21
0270-7306/07/$08.00+0 doi:10.1128/MCB.01246-07

CUB Domain-Containing Protein 1 Is a Novel Regulator of Anoikis Resistance in Lung Adenocarcinoma▽†

Takamasa Uekita,[1] Lin Jia,[1] Mako Narisawa-Saito,[2] Jun Yokota,[3] Tohru Kiyono,[2] and Ryuichi Sakai[1]*

Growth Factor Division,[1] Virology Division,[2] and Biology Division,[3] National Cancer Center Research Institute, 5-1-1 Tsukiji, Chuo-ku, Tokyo 104-0045, Japan

Received 12 July 2007/Returned for modification 31 July 2007/Accepted 16 August 2007

Malignant tumor cells frequently achieve resistance to anoikis, a form of apoptosis induced by detachment from the basement membrane, which results in the anchorage-independent growth of these cells. Although the involvement of Src family kinases (SFKs) in this alteration has been reported, little is known about the signaling pathways involved in the regulation of anoikis under the control of SFKs. In this study, we identified a membrane protein, CUB-domain-containing protein 1 (CDCP1), as an SFK-binding phosphoprotein associated with the anchorage independence of human lung adenocarcinoma. Using RNA interference suppression and overexpression of CDCP1 mutants in lung cancer cells, we found that tyrosine-phosphorylated CDCP1 is required to overcome anoikis in lung cancer cells. An apoptosis-related molecule, protein kinase Cδ, was found to be phosphorylated by the CDCP1-SFK complex and was essential for anoikis resistance downstream of CDCP1. Loss of CDCP1 also inhibited the metastatic potential of the A549 cells in vivo. Our findings indicate that CDCP1 is a novel target for treating cancer-specific disorders, such as metastasis, by regulating anoikis in lung adenocarcinoma.

Src family kinases (SFKs) play important roles in various cell functions, including cell proliferation, cell adhesion, and cell migration, under the control of extracellular stimuli (26). Many studies have shown elevated activity of SFKs or increased protein expression in a variety of human cancers (31). The activities of SFKs often correlate with the malignant potential of cancer and poor prognosis (36). SFKs may contribute to various aspects of tumor progression, including uncontrolled proliferation and migration, disruption of cell-cell contacts, invasiveness, angiogenesis, and resistance to apoptosis.

Anoikis is a form of apoptosis triggered by the loss of cell survival signals generated from interaction with the extracellular matrix (10). Anoikis is considered to be physiologically important in the maintenance of homeostasis and tissue architecture (24). On the other hand, the resistance to anoikis acquired during carcinogenesis has been described as a core aspect of cancer cells for tumor progression and metastasis (12). This property indicates the existence of survival signals in tumor cells, which compensate for similar signals supported by cell-matrix interactions. Since they were originally described by Frisch and Francis (9), several previous reports have shown the crucial role of SFKs in the anoikis resistance of tumor cells. Viral Src oncoprotein abrogates anoikis in epithelial cells (13). Src activation is also important for resistance to anoikis in various cancers, such as colon tumor and lung adenocarcinoma cells (33, 35). However, the exact mechanism that is responsible for the anoikis resistance mediated by SFKs in human cancer cells has not been clearly elucidated.

The purpose of this study, therefore, was to identify the key molecules of anoikis resistance, which mediate signals from activated SFKs in human cancer cells. For that purpose, we analyzed proteins binding to SFKs with and without cell attachment in a number of human lung cancer cell lines. We found that tyrosine phosphorylation of a 135-kDa SFK-binding protein is associated with elevated anchorage independence in a group of lung cancer cell lines, especially in a cell suspension condition. This 135-kDa phosphoprotein was purified and identified as CUB-domain-containing protein 1 (CDCP1) by mass spectrometry. The protein CDCP1 is a type I transmembrane protein that has possible roles in cell-cell and cell-matrix adhesion (3, 5). The molecule has been reported to be highly expressed in lung, breast, and colon cancers (6, 28). Using an RNA interference (RNAi) technique, it was determined that CDCP1 is required for the survival of lung cancer cells both in suspension culture and in soft agar. This study identifies a novel modulator that sustains anoikis resistance under the control of SFKs in lung cancer cells.

MATERIALS AND METHODS

Plasmids, antibodies, and reagents. Full-length cDNA of human CDCP1 with a FLAG tag at the C terminus (wild type [WT]) was obtained by reverse transcription-PCR amplification from the mRNA of A549 human lung adenocarcinoma cells and cloned into pcDNA3.1 (Invitrogen). The cytoplasmic-domain mutants of CDCP1, Y734F (Tyr734 to Phe), Y762F (Tyr762 to Phe), and Y2F (Y734 and Y762 double mutant), were generated by PCR using the overlap extension method of Ho et al. (14). The C2 domain of protein kinase Cδ (PKCδ) corresponding to amino acids (1 to 160) with a hemagglutinin (HA) tag at the C terminus was obtained by PCR and cloned into pcDNA3.1 (Invitrogen). To express the Fyn Src homology 2 (SH2) domain fused with glutathione *S*-transferase (GST) protein (GST-FynSH2), a cDNA fragment of the Fyn SH2 domain corresponding to nucleotides 1018 to 1299 of the reported sequence (GenBank accession number NM 002037) was amplified by PCR and cloned into pGEX4T2 (Amersham Pharmacia).

Antiphosphotyrosine antibody (4G10) and anti-c-Src antibody (clone GD11) were purchased from Upstate Biotechnology. Anti-Akt antibody, anti-phospho-Akt (Ser473) antibody, anti-ERK1/2 antibody (p44/p42 mitogen-activated protein kinase [MAPK] antibody), anti-phospho-ERK1/2 antibody (phospho-p44/p42 MAPK [Thr202/Tyr204] antibody), anti-p38MAPK antibody, anti-phospho-

* Corresponding author. Mailing address: Growth Factor Division, National Cancer Center Research Institute, 5-1-1 Tsukiji, Chuo-ku, Tokyo 104-0045, Japan. Phone: 81-3-3547-5247. Fax: 81-3-3542-8170. E-mail: rsakai@gan2.res.ncc.go.jp.

† Supplemental material for this article may be found at http://mcb.asm.org/.

▽ Published ahead of print on 4 September 2007.

p38MAPK (Thr180/Tyr182) antibody, and anti-phospho-PKCδ (Tyr311) antibody were purchased from Cell Signaling. Anti-HA (Y-11), anti-PKCδ (C-20), and anti-Fyn (FYN3) antibodies were purchased from Santa Cruz Biotechnology. Anti-FLAG antibody (Anti-FLAG M2 peroxidase conjugate specific antibody) and antitubulin antibody (clone B-5-1-2) were purchased from Sigma. The anti-c-Yes antibody was purchased from Transduction Laboratories. An anti-CDCP1 antibody (ab1377) was purchased from Abcam Ltd. To generate the CDCP1 antibody, anti-CDCP1 and the anti-phospho-CDCP1 (Tyr734) antibody were obtained by rabbit immunization using the cytoplasmic domain of CDCP1 fused to GST, and the amino peptides NDSHV(pY^{734})AVIEC of CDCP1 were obtained from MBL Co., Ltd. Horseradish peroxidase (HRP)-conjugated anti-mouse and anti-rabbit antibodies were purchased from Amersham Pharmacia. The HRP-conjugated anti-goat immunoglobulin G (IgG) antibody was purchased from ZYMED. Mouse, rabbit, and goat IgGs were purchased from DakoCytomation. The SFK inhibitor PP2 and the structural analog PP3 were purchased from Calbiochem-Novabiochem Ltd. Etoposide and Rottlerin were purchased from Sigma-Aldrich.

Cell culture and transfection. The human lung adenocarcinoma cell lines A549, PC14, and H322 and human lung squamous carcinoma cell lines H520 and H157 were maintained in RPMI 1640 medium with 10% fetal bovine serum (FBS) at 37°C with 5% CO_2. For transfection, cells were seeded on a cell culture plate or a 2-methacryloyloxyethyl phosphorylcholine (MPC)-coated plate (Nunc) at 1.5×10^5 cells per six wells or 9.0×10^5 cells/10-cm plate, and transfection was performed after 14 h. Expression plasmids were transfected by Lipofectamine 2000 (Invitrogen) according to the manufacturer's instructions. To investigate the effect of PP2 treatment, cells were treated with 10 μM of PP2 or 10 μM of PP3.

Construction of dicer, stealth siRNAs, and miR RNAi vectors. Dicer small interfering RNAs (siRNAs) of human c-Src, Fyn, and c-Yes were generated using the BLOCK-iT RNAi TOPO transcription kit and BLOCK-iT complete dicer RNAi kit (Invitrogen) according to the manufacturer's instructions. In the generation of siRNA for Src, a 726-bp fragment from the initiation codon of human c-Src was chosen as the target sequence and amplified by PCR using the primers forward, 5′-ATGGGTAGCAACAAGAGCAAG-3′, and reverse, 5′-GTGGCACAGGCCATCGGCGTG-3′. As for Fyn and c-Yes, 999-bp and 857-bp fragments were chosen as the target sequences, respectively, and amplified with the following primers: Fyn forward, 5′-ATGGGCTGTGTGCAATGTAGG-3′, and reverse, 5′-CACCACTGCATAGAGCTGGAC-3′; c-Yes forward, 5′-CTGAAAATACTCCAGAGCCTG-3′, and reverse, 5′-CTTTGTCCTAGTTTAACCTCTAG-3′. Dicer siRNA of LacZ was generated by the same procedure as dicer siRNAs of c-Src, Fyn, and c-Yes and was used as a negative control. The stealth siRNAs of human CDCP1, PKCδ, and the negative control were ordered from Invitrogen. Specific primers were as follows: CDCP1 forward, 5′-GCUCUGCCACGAGAAAGCAACAUUA-3′, and reverse, 5′-UAAUGUUGCUUUCUCGUGGCAGAGC-3′; PKCδ forward, 5′-GGUGCAGAAGAAGCCGACCAUGUAU-3′, and reverse, 5′-AUACAUGGUCGGCUUCUUCUGCACC-3′. Transfection of both dicer and stealth siRNAs was performed with Lipofectamine 2000 (Invitrogen), and the effect was analyzed less than 48 h after the transfection.

A system stably expressing siRNA was generated using the BLOCK-iT Pol II miR RNAi expression vector kit (Invitrogen) according to the manufacturer's instructions. In the generation of the miR RNAi vector for humans, CDCP1 was chosen as the target sequence, using the forward primer 5′-TGCTGAATGTTGCTTTCTCGTGGCAGGTTTTGGCCACTGACTGACCTGCCACGAAAGCAACATT-3′ and the reverse primer 5′-CCTGAATGTTGCTTTCGTGGCAGGTCAGTCAGTGGCCAAAACCTGCCACGAGAAAGCAACATTC-3′. Cells stably expressing the miR RNAi vector for CDCP1 and LacZ were established and cultured in medium containing blasticidin (Invivogen) at a concentration of 10 μg/ml for 3 weeks. Two clones expressing the CDCP1 RNAi vector (miCDCP1-1 and -2) were selected by significant suppression of the CDCP1 protein (<10%), and two clones from the control LacZ vector were also selected (miLacZ-1 and -2).

Soft-agar colony assay. Six-well tissue culture plates were coated with a layer of RPMI 1640-10% FBS containing 0.5% ultrapure agarose (Invitrogen). Subconfluent A549 cells transfected with the dicer siRNA or miR RNAi vector-expressed clone were treated with EDTA, washed in phosphate-buffered saline twice, and resuspended in RPMI 1640-10% FBS at 6×10^3 cells/ml. Then, a 500-μl cell sample was added to 1 ml of RPMI 1640-10% FBS containing 0.5% ultrapure agarose (final concentration, 0.33%). The cells were plated on the coated tissue culture plates, allowed to solidify, and then placed in a 37°C incubator. After 30 days, colonies were scanned using a GS-800 calibrated densitometer (Bio-Rad), and the numbers of colonies per well were determined. Soft-agar assays were performed three times.

Immunoprecipitation and Western blotting. Cell lysates were prepared with protease inhibitors in PLC buffer (10 mM Tris-HCl, pH 7.5, 5 mM EGTA, 150 mM NaCl, 1% Triton X-100, 10% glycerol, 10 μg/ml aprotinin, 1 mM sodium orthovanadate [Na_3VO_4], and 100 μg/ml leupeptin). The protein concentration was measured by BCA protein assay (Pierce). For purification, 1 μg of monoclonal or affinity-purified polyclonal antibody was added to the proteins, which were then incubated with 500 μl (2 mg/ml) of cell lysate for 2 h at 4°C. Next, they were precipitated with protein A- or protein G-agarose for 1 h at 4°C. The immunoprecipitates were extensively washed with PLC buffer and prepared for Western blotting.

For Western blotting, samples were separated on sodium dodecyl sulfate-polyacrylamide gel electrophoresis and transferred to a polyvinylidene difluoride membrane (Immobilon-P; Millipore). After blocking of the membrane with blocking buffer (Blocking One; Nakarai Tesque), the membrane was probed with antibodies for detection. The membrane was further probed with HRP-conjugated anti-mouse, anti-rabbit, or anti-goat IgG (1:4,000) to visualize the reacted antibody.

Images were captured by a molecular imager (GS-800; Bio-Rad), and the density of each smear was quantified using Quantity One software (Bio-Rad).

Identification of CDCP1. Isolated GST-FynSH2 protein coupled with cyanogen bromide (CNBr) was used to purify the 135-kDa and 70-kDa proteins from the A549 cells cultured for 48 h on MPC-coated plates in growth medium. Briefly, ~3×10^7 suspended A549 cells in a total of 400 dishes (10-cm dish; 30 ml culture medium) were collected and lysed in PLC buffer. The cell lysate was rotated for 8 h at 4°C with GST-FynSH2 protein and washed four times using PLC buffer before being eluted with GST-FynSH2-coupled proteins using 8 M urea buffer (8 M urea, 10 mM Tris-HCl, pH 7.4, 150 mM NaCl, 1% Triton X-100). Secondly, the eluted sample was dialyzed three times against a 100-fold volume of dialysis buffer (10 mM Tris-HCl, pH 7.4, 150 mM NaCl, 1 mM Na_3VO_4), and then the sample was affinity purified with antiphosphotyrosine monoclonal antibody (4G10) coupled with CNBr. 4G10-coupled proteins were washed four times using PLC buffer and once using heptyl-glucoside buffer (10 mM Tris-HCl, pH 7.4, 150 mM NaCl, 0.1% heptyl-glucoside). Next, the samples were eluted using 0.1 M phenylphosphate in heptyl-glucoside buffer. The purified 135-kDa and 70-kDa proteins were concentrated, electrophoresed, and blotted onto a ProBlott membrane (Applied Biosystems). After visualization with colloidal gold total-protein stain (Bio-Rad), the isolated 135-kDa and 70-kDa bands were analyzed by mass spectrometry. Four sets of amino acid sequences determined from the 135-kDa band and an amino acid sequence determined from the 70-kDa band indicated that both the 135-kDa and 70-kDa proteins were CDCP1.

Apoptosis assay. Each cell was treated with EDTA, and 1×10^4 cells were reseeded onto normal or MPC-coated 96-well plates. After 24 h, the cells were lysed and used for the detection of apoptosis. Apoptosis levels were determined using a cell death ELISA kit (Roche Molecular Biochemicals), which detects the presence of nucleosomes in the cytoplasm of apoptotic cells. The absorbance of the samples was measured at a wavelength of 405 nm using a microplate reader model 550 (Bio-Rad).

BrdU incorporation assay. Cell proliferation was analyzed with the cell proliferation ELISA BrdU kit according to the manufacturer's instructions (Roche Molecular Biochemicals) based on the measurement of 5-bromo-2′-deoxyuridine (BrdU) incorporation during DNA synthesis of proliferating cells. Briefly, A549 cells were cultured in triplicate for 24 h in 96-well plates (1.0×10^4 cells/well) with or without cell attachment. The cells were subjected to BrdU incorporation for 6 h. The colorimetric change was measured at 450 nm on a microplate reader model 550 (Bio-Rad).

Infection of retroviral constructs. The retroviral vectors PQCXIN (Clontech) and pCMSCVbsd were used to express human CDCP1 (WT) and Y734F with a FLAG tag at the C terminus and full-length cDNA of Fyn kinase with a double HA tag at the C terminus (FynHA), respectively. pCMSCVbsd contains the blasticidin resistance gene in place of the puromycin resistance gene of pCMSCVpuro (20). These retrovirus vectors were converted into the destination vectors with a vector conversion kit (Invitrogen). The cDNA segments were first cloned into pDONR221 and then into the destination vector, pDEST-PQCXIN or pDEST-CMSCVbsd, according to the manufacturer's instructions (Invitrogen). The production of recombinant retroviruses was performed as described previously (25). Briefly, the retroviral vector and the packaging construct pCL-10A1 were cotransfected into 293T cells using TransIT-293 (Mirus Co., Madison, WI) according to the manufacturer's instructions, and culture fluid was harvested 48 to 72 h posttransfection. H322 cells were infected with the viral fluid in the presence of 4 mg/ml Polybrene, and the infected cells were selected in the presence of 800 μg/ml G418 or 5 μg/ml blasticidin. For combinations of retroviral infections, cells were first transduced with CDCP1 and then with Fyn kinase.

Experimental metastasis assay. Female BALB/cAJcl-nu/nu nude mice were purchased from CLEA Japan Inc. All of the mice used in these experiments were

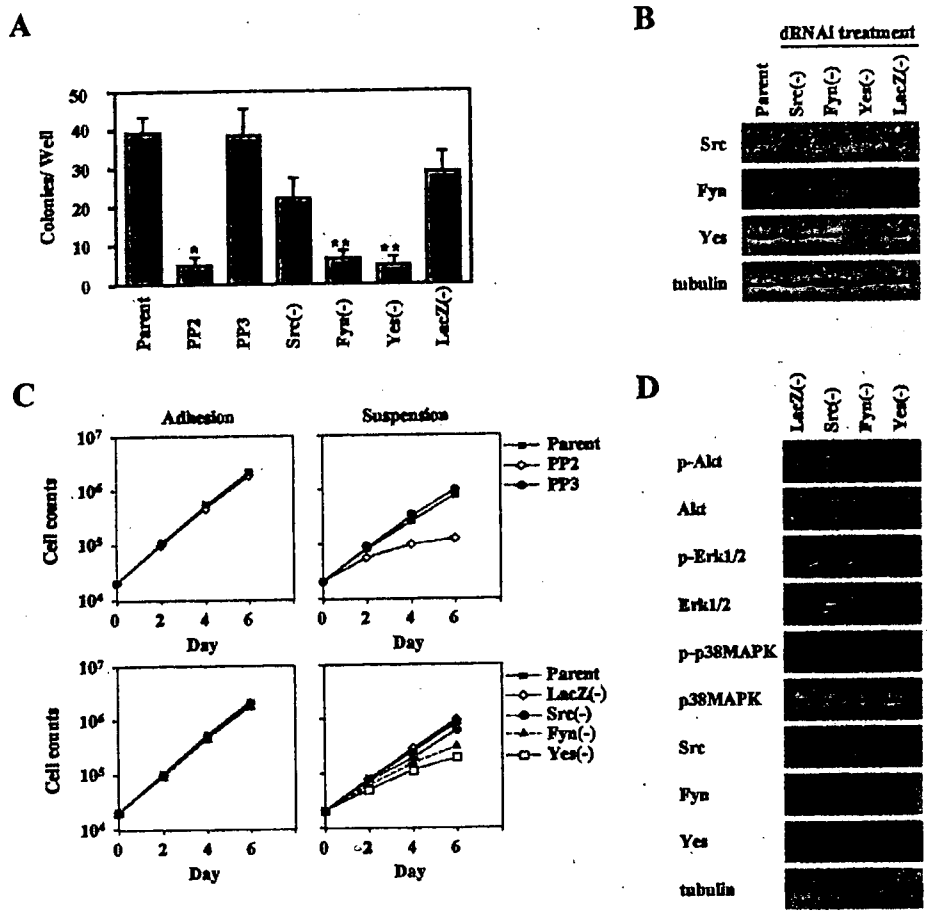

FIG. 1. Anchorage independence of lung adenocarcinoma cells requires SFK. (A) The effect of SFKs on anchorage independence was determined by soft-agar assay. A549 cells were treated with the SFK inhibitor PP2 (10 μM) and SFK dicer RNAi [bars Src(−), Fyn(−), and Yes(−)], and controls [bars Parent, PP3, and LacZ(−)] were seeded onto each soft-agar plate (3×10^3 cells). Colonies equal to and larger than 0.5 mm in diameter were counted after 30 days. The error bars represent standard deviations, and the asterisk indicates statistically significant differences ($P < 0.01$) between the parent and PP2 treatment cells, while the double asterisk indicates statistically significant differences ($P < 0.01$) between LacZ(−) and each of the SFK RNAi treatment cells. (B) A549 cells transiently transfected with c-Src, Fyn, c-Yes, or LacZ dicer RNAi (dRNAi) were incubated for 48 h in culture plates. The cells were lysed and subjected to immunoblotting with the indicated antibodies. (C) Cell growth in A549 cells was subjected to a determination of the number of cells, as described for panel A. Approximately 2×10^4 cells were seeded onto normal (Adhesion) or MPC-coated (Suspension) culture plates with medium. The growth medium was changed every 2 days. The total cell number on each plate was determined every 2 days by a Coulter particle counter z1 (Beckman). (D) SFKs did not affect the phosphorylation of Akt, Erk1/2, or p38MAPK. The lysate of suspended A549 cells transiently transfected with dicer RNAi for each of the SFKs was prepared and subjected to immunoblotting with the indicated antibodies.

6 to 8 weeks old. A549 clones generated by the miR RNAi system and H322 cells were evaluated by experimental metastasis assay, as described by Fidler et al. (8). Briefly, cells (5×10^5 cells/0.2 ml of medium without serum; $n = 6$) were injected into the tail veins of mice. The mice were sacrificed 100 days after cell inoculation for the counting of metastatic nodules. The numbers of lung metastases and nodule formations were determined.

To determine the effect of CDCP1 on tumor growth in nude mice, A549 clones (3×10^6 cells/0.2 ml of medium without serum) were subcutaneously injected into the right flanks of mice. The mice were killed at 30 days. The results are expressed as the mean weight of tumors from three mice ± standard error.

RESULTS

The anchorage independence of lung cancer cells involves SFKs. We first examined the involvement of SFKs in the anchorage independence of A549 lung adenocarcinoma cells using the colony formation assay on soft agar with or without PP2, an SFK inhibitor (Fig. 1A). A549 cells and cells treated with PP3, an inactive derivative of PP2, formed a similar number of colonies in soft agar, while the addition of PP2 caused a significant decrease in the numbers of colonies. A similar effect of PP2 was observed in most lung cancer cells, such as the PC3, PC14, H520, and LK2 cell lines (data not shown).

To determine which member of the SFKs mainly contributes to the anchorage independence of A549 cells, individual expression of c-Src, Fyn, and c-Yes was downregulated using RNAi technology (Fig. 1B), and colony formation assays were performed on soft agar (Fig. 1A). A549 cells treated with Fyn or c-Yes siRNAs formed significantly fewer colonies than the control cells treated with LacZ siRNA, while cells treated with c-Src siRNA formed slightly fewer colonies. We also observed

a similar suppressive effect of Fyn and c-Yes RNAi in PC14 and H520 lung cancer cells (data not shown).

To further assess the significance of SFKs during the anchorage-independent growth, the effects of PP2 or RNAi for each SFK on cell growth were examined with or without cell attachment using a normal culture dish or MPC-coated dish, respectively. In adherent culture, no significant effect on cell numbers was observed by treatment with PP2 or by any siRNA for the SFKs (Fig. 1C, Adhesion). In suspension culture, however, A549 cells treated with PP2 or with siRNAs for Fyn or c-Yes showed a significant reduction of cell counts compared with untreated cells, while cells treated with c-Src siRNA showed only a slight reduction in cell numbers (Fig. 1C, Suspension). Neither control siRNA nor PP3 had a detectable effect on cell growth in suspension culture.

The phosphatidylinositol (PI) 3-kinase/Akt pathway and the MAPK pathway are the most significant pathways mediating growth factor signals during cell survival and cell proliferation. We therefore examined whether downstream signals of SFKs, which lead to anchorage independence of A549 cells, involve the activation of these two pathways. Suppression of the expression of c-Src, Fyn, or c-Yes by each RNAi had no significant effects on the phosphorylation of Akt and ERK in the suspension culture of A549 cells. These sets of siRNAs also had no effect on the phosphorylation of p38MAPK (Fig. 1D).

Taken together, these data suggest that Fyn and c-Yes are required for anchorage independence in A549 cells, and the cellular signals mediated by these kinases are independent of the Akt, ERK, and p38MAPK pathways.

Purification of 135-kDa and 70-kDa phosphotyrosine proteins associating with SFKs in suspension culture. To identify which molecules mediate the SFK signals specific for anchorage independence, we analyzed the phosphotyrosine-containing proteins that bind to SFKs. Among the proteins associated with SFKs, two proteins with molecular masses of 135 kDa and 70 kDa were prominently phosphorylated, even in suspension culture (Fig. 2A), and these proteins were also phosphorylated in PC14 and H520 cell lines, which also exhibit a high level of anchorage independence (Fig. 2A, High). In contrast, the H322 and H157 cell lines, which formed a small number of colonies in soft agar (Fig. 2A, Low), displayed rather lower levels of phosphorylation of these two proteins (Fig. 2A). Using these results, we sought to identify proteins that function as downstream mediators of SFKs in anchorage-independent growth.

As several antibodies against the known phosphoproteins failed to recognize the 135-kDa and 70-kDa proteins, we applied affinity purification. Using A549 cells cultured for 48 h with and without cell attachment, these 135-kDa and 70-kDa proteins were pulled down with the Fyn SH2 domain more efficiently under suspension conditions (Fig. 2B). A total of $\sim 1.2 \times 10^{10}$ cells in suspension culture were first purified with the Fyn SH2 domain. After purification by a second affinity column using a 4G10 antiphosphotyrosine antibody, samples were analyzed by Western blotting (Fig. 2C, WB) and colloidal gold total-protein stain (Fig. 2C, G). Bands corresponding to the two proteins were cut out and analyzed by mass spectrometry. Four peptides from the 135-kDa band and one peptide from the 70-kDa band were determined by mass spectrometry to be the recently identified membrane protein CDCP1 (Fig. 2C). The proteins at molecular masses of both 135 kDa and 70 kDa in the suspension culture appeared to contain the single protein CDCP1. The 70-kDa protein was estimated to be a cleaved product of 135-kDa CDCP1, as previously reported (5).

Identification of the major phosphoprotein of the 135-kDa and 70-kDa proteins as CDCP1 and its association with anchorage independence. Anti-CDCP1 antibody recognized proteins of exactly the same molecular masses as the 135-kDa and 70-kDa proteins both in the whole-cell lysate and in the sample pulled down by the Fyn SH2 domain (Fig. 3A, WCL and PD). CDCP1 was also clearly coimmunoprecipitated with each SFK molecule originally expressed in A549 cells, especially with Fyn and c-Yes, which is consistent with the original 135-kDa protein (Fig. 3A, IP). On the other hand, immunoprecipitation with anti-CDCP1 antibody revealed that CDCP1 was strongly associated with Fyn and c-Yes and very weakly with c-Src (Fig. 3B).

To confirm that the phosphorylation of CDCP1 in each lung cancer cell line is associated with high anchorage independence, we generated a phosphospecific antibody (p-CDCP1 [Tyr734]) against tyrosine 734 of CDCP1, which is reported to be a major phosphorylation site for SFK (1, 5), and analyzed the phosphorylation of CDCP1 in each cell line (Fig. 3C). Prominent phosphorylation of CDCP1 was observed in the A549, PC14, and H520 lung cancer cells with high anchorage independence (Fig. 3C, High), while the H322 and H157 cells, which have low anchorage independence (Fig. 3C, Low), exhibited rather low levels of phosphorylation of CDCP1. From these results, we concluded that the 135-kDa phosphoprotein detected in lung cancer cells is CDCP1, and its phosphorylation status appears to be associated with anchorage independence.

We examined whether the phosphorylation of CDCP1 is altered with or without cell attachment in the culture. After detachment of A549 cells with EDTA, the cells were either plated on a normal dish to cause readhesion or plated on an MPC-coated dish to grow in suspension for 48 h. Under either plating condition, the phosphorylation level of CDCP1 was continuously increased until 24 h; however, it exhibited a sudden decrease at 48 h in adhesion culture, while it increased further in suspension culture (Fig. 3D). Notably, these dynamic changes of phosphorylation during cell suspension and readhesion appear to partially reflect the change in the expression level of CDCP1.

CDCP1 is a regulator of anoikis resistance in lung adenocarcinoma. Next, we checked whether CDCP1 is involved in the regulation of the anchorage independence of A549 cells under the control of SFK activity. For this purpose, we obtained the stable A549 cell clones miCDCP1-1 and miCDCP1-2, which showed suppressed expression of the CDCP1 protein, by using the siRNA for CDCP1 with a BLOCK-iT Pol II miR RNAi expression vector system (Fig. 4A). Both of the clones formed significantly fewer colonies in the soft-agar assay than the LacZ clones (Fig. 4B), suggesting that CDCP1 is actually required for the anchorage independence of A549 lung adenocarcinoma.

Anchorage independence may reflect the persistence of growth and/or survival of cancer cells in suspension; therefore, the effects of CDCP1 expression in suspended cells on cell

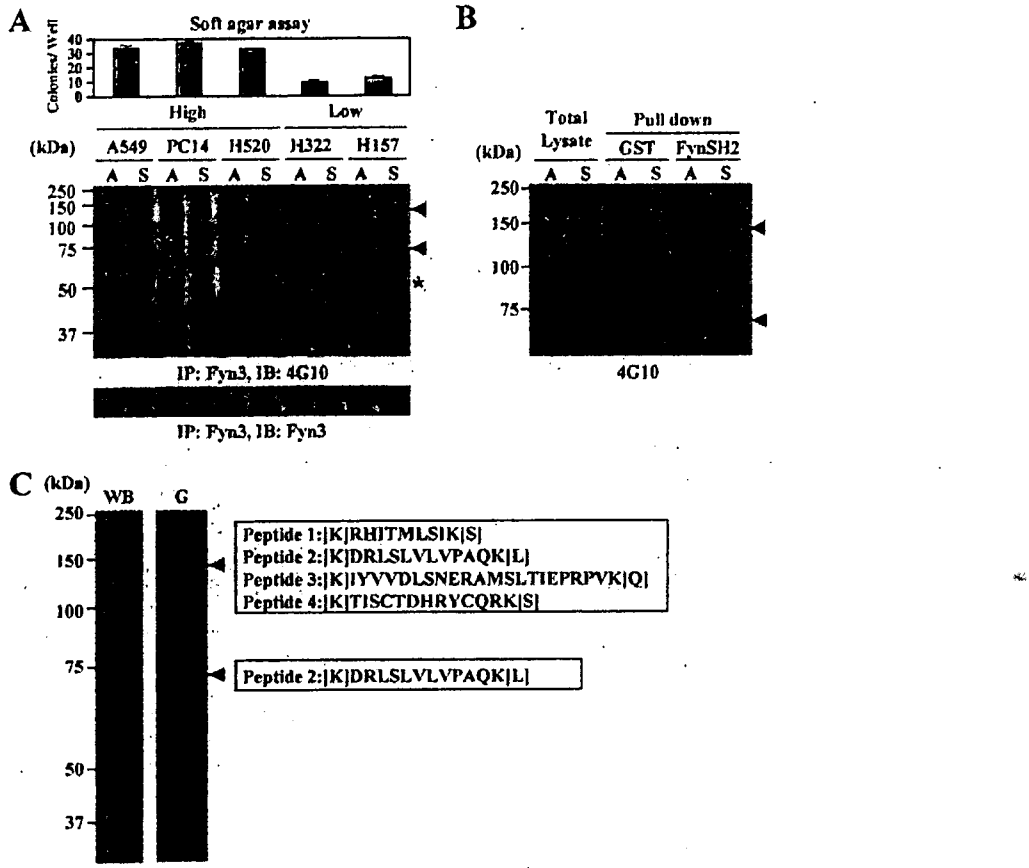

FIG. 2. Purification of phosphotyrosine-containing 135-kDa and 70-kDa protein-forming complexes with SFKs in suspension culture. (A) Anchorage independence in a series of lung cancer cell lines was examined by soft-agar assay (top). The large number of colonies formed in the lung cancer cell lines A549, PC14, and H520 (High) and the small number of colonies formed in the H322 and H157 cell lines (Low) cultured for 48 h under both adhesion and suspension conditions were collected and subjected to immunoprecipitation (IP) with anti-Fyn (Fyn3) antibody and immunoblotting (IB) with antiphosphotyrosine (4G10) antibody. Phosphotyrosine-containing proteins coimmunoprecipitated with Fyn at the molecular masses of 135 kDa and 70 kDa are indicated by arrowheads. The asterisk indicates phosphorylated Fyn. The expression of Fyn in each cell lysate was confirmed by immunoblotting (bottom). A, adhesion; S, suspension. The error bars represent standard deviations. (B) GST-FynSH2 protein generated by *Escherichia coli* was used to pull down the lysate of A549 cells cultured under adhesion or suspension conditions. The isolated samples were immunoblotted with antiphosphotyrosine (4G10) antibody. The arrowheads indicate the phosphotyrosine-containing 135-kDa and 70-kDa proteins. (C) Phosphotyrosine-containing proteins (135 kDa and 70 kDa) were purified according to the protocol described in Materials and Methods. Aliquots of the purified 135-kDa and 70-kDa phosphotyrosine-containing proteins were examined by Western blotting (WB) using antiphosphotyrosine (4G10) antibody, and the remaining samples were stained with colloidal gold total-protein stain (G). Four peptides determined by mass spectrometry (peptides 1 to 4) were identified within the sequence of CDCP1.

proliferation and on cell apoptosis were individually examined. Each miCDCP1 clone in suspension culture showed an increased level of apoptosis compared with miLacZ clones (Fig. 4C). In contrast, no significant change in the cell growth level was observed in each of the miCDCP1 and miLacZ clones compared with the parental A549 cells in suspension culture (Fig. 4D). Importantly, there was no significant change in either cell growth or apoptosis in the adhesion culture (Fig. 4C and D).

We also examined the effect of the expression of phosphorylated CDCP1 on cell proliferation and cell apoptosis using H322 lung adenocarcinoma cells with low anchorage independence. CDCP1 (WT) and/or Fyn kinase with double HA tags at the C terminus (FynHA) were expressed in H322 cells by retroviral vectors, and the expression was checked by Western blotting (Fig. 5A). Additionally, a CDCP1 mutant lacking a putative SFK-binding site (Y734F) was also expressed (2). An increased level of phosphorylation of CDCP1 was observed in H322 cells overexpressing both WT and Fyn kinase (Fig. 5A, WT+FynHA), which caused an inhibition of apoptosis in suspension culture (Fig. 5B). These changes were not observed with either Fyn kinase or WT CDCP1 alone. On the other hand, expression of Y734F alone increased the level of apoptosis in suspension culture, suggesting a dominant-negative effect of this CDCP1 mutant (Fig. 5B, Y734F). A slight enhancement of cell proliferation in suspension culture was observed by expressing Fyn kinase and either WT or mutant CDCP1, but this change was not significant (Fig. 5C).

These results suggest that phosphorylation of CDCP1 confers anchorage independence through the inhibition of apoptosis. In other words, phosphorylation of CDCP1 regulates resistance to anoikis in lung cancer cells.

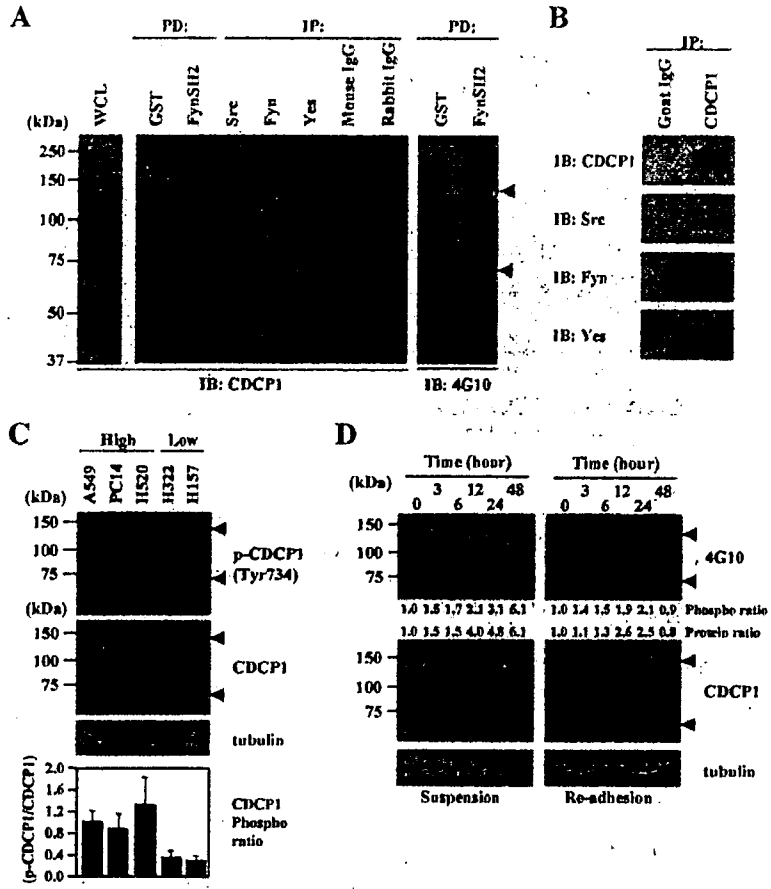

FIG. 3. Identification of the 135-kDa and 70-kDa proteins as CDCP1 and its phosphorylation associated with anchorage independence. (A) The lysate of A549 cells was subjected to whole-cell lysate (WCL) or pull-down assay with GST-FynSH2 protein (PD) or immunoprecipitated with anti-c-Src, anti-Fyn, and anti-c-Yes antibodies (IP) and immunoblotted (IB) with anti-CDCP1 antibody. The same blot was rehybridized with antiphosphotyrosine (4G10) antibody. (B) The lysate of A549 cells was immunoprecipitated with anti-CDCP1 antibody (ab1377) or goat IgG as indicated. The precipitates were subjected to immunoblotting with anti-c-Src, anti-Fyn, anti-c-Yes, and anti-CDCP1 antibodies. (C) The large number of colonies formed by the lung cancer cell lines A549, PC14, and H520 (High) and the small number of colonies formed by the H322 and H157 cell lines (Low) cultured for 48 h in the suspension condition were collected and subjected to immunoblotting with anti-phospho-CDCP1 (Tyr734) and CDCP1 antibodies. This experiment was performed three times. The ratio of the phosphorylation level in each lung adenocarcinoma cell was measured as described in Materials and Methods. The error bars represent standard deviations. (D) Time course analysis of CDCP1 expression and phosphorylation with or without cell attachment. A549 cells were reseeded on normal cell culture plates and an MPC-coated plate at a density of 1.5×10^5 cells per plate with complete medium. For the preparation of the reseeding cells, 2 mM EDTA/Hanks' balanced salt solution was used to detach the cells. For each time point, cells were collected and subjected to immunoblotting with the indicated antibody. The same membrane rehybridized with antitubulin antibody confirmed the concentration of total proteins in each lysate (tubulin). The arrowheads indicate CDCP1.

PKCδ is a signal molecule downstream of CDCP1 during anoikis resistance in lung adenocarcinoma. CDCP1 protein has been shown to bind PKCδ in a phosphorylation-dependent manner (2). PKCδ is a regulator of apoptosis, and it has been reported that the phosphorylation of PKCδ requires the activity of SFKs (37). By treatment with the SFK inhibitor PP2, both the association of PKCδ with CDCP1 and the phosphorylation of PKCδ at Tyr311 were clearly inhibited (Fig. 6A). CDCP1 (WT) and the CDCP1 protein with a point mutation at Tyr734 (Y734F) were C-terminally FLAG tagged and expressed in COS7 cells. After transfection with each plasmid, the association of the Fyn SH2 domain with WT and Y734F mutants was examined. The Fyn SH2 domain was able to pull down the WT but not the Y734F mutants (Fig. 6B, PD: Fyn SH2). The levels of tyrosine phosphorylation of Y734F mutants was much lower than that of the WT in A549 cells (Fig. 6B, IB: 4G10), suggesting that Tyr734 of CDCP1 directly binds to Fyn and that the association is essential for the phosphorylation of CDCP1. The association between CDCP1 and PKCδ was also impaired in the Y734F mutant compared with the WT, indicating that the phosphorylation of CDCP1 is required for the association.

Overexpression of Y734F in A549 cells also blocked the association between PKCδ and CDCP1 and the phosphorylation of PKCδ at Tyr311 (Fig. 6B). Moreover, treatment with CDCP1 siRNA also decreased the phosphorylation level of PKCδ (Fig. 6C). In addition, the phosphorylation level of PKCδ at Tyr311 was elevated in H322 cells by overexpressing both WT CDCP1 and Fyn kinase but not significantly with either the WT, the Y734F mutant, or Fyn kinase alone (see the

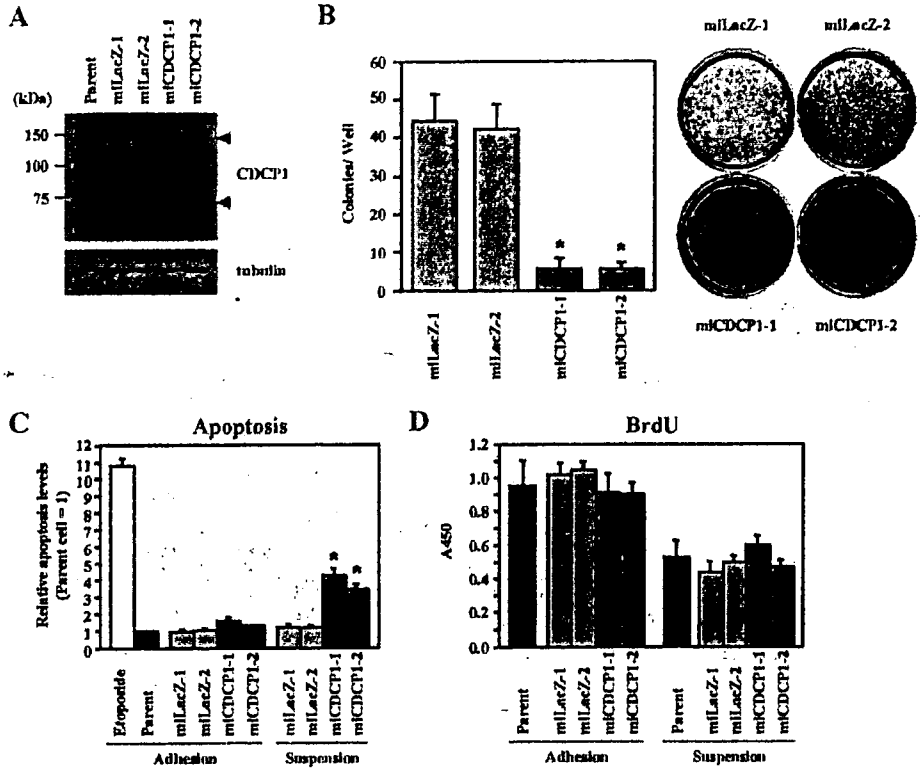

FIG. 4. CDCP1 confers anchorage independence by inhibiting apoptosis in suspended lung adenocarcinoma. (A) CDCP1-defective A549 cell clones (miCDCP1-1 and miCDCP1-2) were generated by an miR RNAi expression vector kit (Invitrogen). miLacZ-1 and miLacZ-2 were control clones. The expression of CDCP1 in each clone (1.5×10^5 cells) cultured for 24 h in an MPC-coated plate was examined by Western blotting using CDCP1 antibody. The concentration of total protein in each clone was confirmed by the same membrane rehybridized with antitubulin antibody (bottom). The arrowheads indicate CDCP1. (B) Each CDCP1-defective clone and control clone was seeded onto soft-agar plates (3×10^3 cells) (right). Colonies equal to and larger than 0.5 mm in diameter were counted after 30 days. The error bars represent standard deviations, and the asterisks indicate statistically significant differences ($P < 0.01$) (left). (C) CDCP1-defective A549 cell clones (miCDCP1-1 and -2) and control miLacZ clones (1.0×10^4 cells) were cultured in normal and MPC-coated 96-well plates. After 24 h, the cells were lysed and apoptosis was examined using a cell death ELISA kit (Roche). The total apoptotic level of A549 cells was examined by treatment with etoposide (25 μM). The relative apoptosis levels are shown as the levels of apoptosis in each clone compared with those of parental cells. In suspension culture, miCDCP1 clones exhibited an increased level of apoptosis compared with that of miLacZ clones. The error bars represent standard deviations, and the asterisks indicate statistically significant differences ($P < 0.01$). (D) Cell proliferation was determined with a cell proliferation ELISA BrdU kit (Roche). Each clone (1.0×10^4 cells) was cultured on normal and MPC-coated 96-well plates. No significant change in cell proliferation was observed in the miCDCP1 or in miLacZ clones compared with parental A549 cells with or without cell attachment. The error bars represent standard deviations.

supplemental material). Therefore, CDCP1 might be required for the phosphorylation of PKCδ by linking PKCδ to SFKs in a phosphorylation-dependent manner.

To check whether PKCδ can regulate anoikis in lung adenocarcinoma cells, cell apoptosis caused by the suspension of miCDCP1 and miLacZ clones was examined with or without PKCδ RNAi. As shown in Fig. 6D, PKCδ RNAi increased the level of apoptosis in the control A549 cells (miLacZ) to a degree similar to that achieved by the suppression of CDCP1 expression (miCDCP1); however, no additive effect on cell apoptosis was observed by the suppression of both CDCP1 and PKCδ. Similar results were obtained from two other independent sets of siRNAs for PKCδ (data not shown). Moreover, treatment with the PKC inhibitor Rottlerin increased the level of apoptosis compared with the parental A549 cells (Fig. 6E). We also examined whether the blocking of the CDCP1-PKCδ signal pathway affects anoikis resistance in A549 cells by overexpressing the C2 domain of PKCδ, which has been shown to be responsible for the association with tyrosine-phosphorylated CDCP1 (2). The HA-tagged C2 domain of PKCδ (C2HA) expressed in A549 cells was actually associated with phosphorylated CDCP1 (Fig. 6F, upper panel) and suppressed the tyrosine phosphorylation levels of PKCδ (Fig. 6F, bottom). At the same time, overexpression of C2HA resulted in a significant increase in the level of apoptosis in suspension culture compared with a mock-transfected control, while it had no significant effect on adherent culture (Fig. 6G).

These results suggest that the CDCP1-SFK complex is required for the phosphorylation of PKCδ under suspension conditions and that PKCδ is a signal molecule for regulating anoikis resistance downstream of CDCP1 signaling.

CDCP1 affects the metastatic potential of A549 lung adenocarcinoma in vivo. Anchorage independence is thought to be an important characteristic of cancer cells that acquire metastatic potential. In order to determine the effect of CDCP1 for in vivo metastasis, miCDCP1 and miLacZ cells were injected

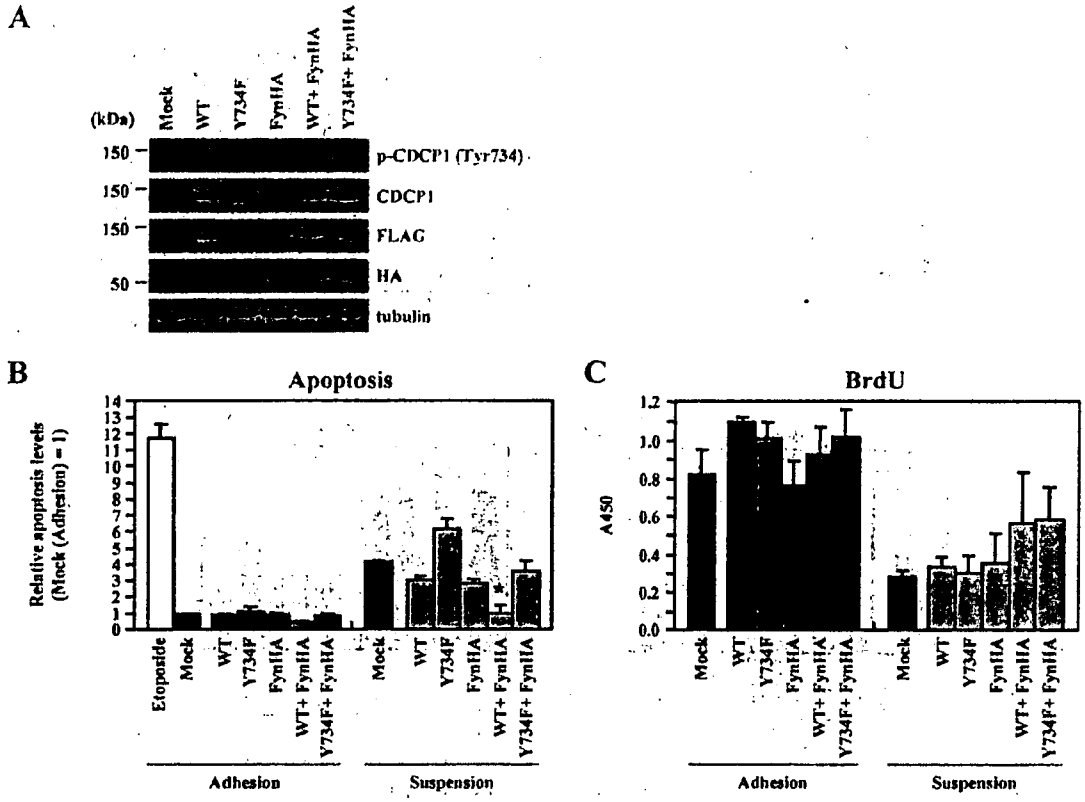

FIG. 5. Anoikis resistance was recovered by phosphorylated CDCP1 in H322 cells with low anchorage independence. (A) H322 cells that overexpressed CDCP1 (WT), a CDCP1 mutant (Y734F), and/or Fyn kinase tagged with HA (FynHA) was incubated for 24 h in MPC-coated plates. The cells were lysed and subjected to immunoblotting with the indicated antibodies. (B) Cells, as indicated (1.0×10^4 cells), were cultured in normal and MPC-coated 96-well plates. After 24 h, the cells were lysed and apoptosis was examined using a cell death ELISA kit (Roche). The total apoptotic level of mock-infected cells was examined by treatment with etoposide (25 μM). The relative apoptosis levels are shown as the levels of apoptosis in each of the cells compared with mock-infected cells in adhesion culture. The error bars represent standard deviations, and the asterisk indicates a statistically significant difference ($P < 0.05$) between mock-transfected cells and other cells in suspension culture. (C) Cell proliferation was determined with a cell proliferation ELISA BrdU kit (Roche). Each of the cells (1.0×10^4 cells) was cultured on normal and MPC-coated 96-well plates. No significant change in cell proliferation was observed in each of the cells compared with mock-infected cells with or without cell attachment (BrdU). The error bars represent standard deviations.

into the tail veins of mice and raised for 100 days. The metastatic capacity was assessed from the number of metastatic cell nodules in mouse lungs. The frequency and number of the metastatic nodules observed in the lungs of each miCDCP1 clone were much less than those found in A549 miLacZ (Fig. 7B). Additionally, H322 cells that belong to the group with low anchorage independence displayed metastasis in only one out of six mice. The average of each of the metastatic nodules and the results of metastasis for each mouse are shown in Table 1. Interestingly, no significant change in tumor growth in nude mice was observed in the miCDCP1-1 clone compared with the A549 miLacZ-1 clone (Fig. 7A). Since the metastatic assay mimics only the middle and late processes of metastasis, these results indicate that CDCP1 affects the later process in the metastasis of lung adenocarcinoma in vivo, possibly through the regulation of anchorage independence.

DISCUSSION

This study has identified CDCP1 as a crucial regulatory molecule of anoikis resistance in lung cancer cells. The signal mediated by the CDCP1-SFK complex appears to play the principal role in overcoming anoikis. CDCP1 has previously been identified as a novel epithelial tumor antigen (28) and as a tumor-associated protein preferentially expressed by highly metastatic epidermoid carcinoma (15), although little is known about the function of CDCP1 in tumor cells. Some putative functions have been suggested, such as the hypothesis that CDCP1 is a mitotic substrate of SFKs under cell cycle regulation in MDA-468 breast cancer cells (3). In this study, we found a distinct novel function of CDCP1 in tumor cells that occurs through phosphorylation by SFKs.

We found that the disruption of CDCP1 expression in A549 cells resulted in defective colony formation in soft agar, suggesting that CDCP1 affects anchorage independence (Fig. 4B). Anchorage independence is an outstanding characteristic of tumor cells, which confers the ability to grow without attachment to the extracellular matrix. Anchorage independence may come from either persistent cell growth or resistance to apoptosis in a suspension condition. As found in this study, CDCP1 does not significantly affect cell growth. A key finding here is that the loss of CDCP1 induces the apoptosis of lung